



Reconstructing the Late Pleistocene – Anthropocene interaction between the neotectonic and archaeological landscape evolution in the Apennines (La Sassa cave, Italy)

L. Alessandri ^{a,1,*}, G.L. Cardello ^{b,c,1}, P.A.J. Attema ^a, V. Baiocchi ^d, F. De Angelis ^e, S. Del Pizzo ^f, F. Di Ciaccio ^f, A. Fiorillo ^g, M. Gatta ^{g,h}, F. Monti ^d, M. Onori ^d, M.F. Rolfo ^g, M. Romboni ^e, G. Sottili ^c, S. Troisi ^f

^a University of Groningen, GIA, Poststraat 6, 9712ER, Groningen, the Netherlands

^b Department of Chemistry and Pharmacy, University of Sassari, Italy

^c Sapienza University of Rome, Earth Sciences Department, Piazzale Aldo Moro 5, 00185, Roma, Italy

^d Sapienza University of Rome, DICEA, Via Eudossiana 18, 00184, Rome, Italy

^e University of Tor Vergata, Centre of Molecular Anthropology for Ancient DNA Studies, Via Della Ricerca Scientifica 1, 00133, Rome, Italy

^f Parthenope University of Naples, Centro Direzionale Isola C4, Naples, Italy

^g University of Tor Vergata, Department of History, Culture and Society, Via Columbia 1, 00133, Rome, Italy

^h University of York, Department of Archaeology, King's Manor, Exhibition Square, York, YO1 7EP, UK

ARTICLE INFO

Article history:

Received 28 April 2021

Received in revised form

23 June 2021

Accepted 24 June 2021

Available online xxx

Handling Editor: Dr Mira Matthews

Keywords:

Neotectonics

Apennines

Pleistocene

Copper age

Early and middle bronze age

Landscape archaeology

Protoapenninico and grotta nuova

ABSTRACT

Caves are one of the most conservative environments on Earth, where archaeological, anthropological, climatic and tectonic data can be well-preserved. Here, we present the results of a multidisciplinary method that allowed us to recognize, for the first time in this area, the interaction between Late Pleistocene to Anthropocene neotectonic and archaeological evolutionary stages of a cave of the Apennines (La Sassa cave), that encompass also its surroundings (Volsci Range and Pontina Plain). Both structural and 3D survey highlighted a step-wise shape of the cave due to normal fault steps that allowed the localized formation of concretions also enveloping archaeological layers. Sixteen ¹⁴C ages on fauna and human bones and thousands of archaeological finds provided chronological constraints of faulting in the Late Pleistocene and possibly also after the Middle Bronze Age. In the frame of a region that was not previously recognized as tectonically active, the structural evidence is relevant for understanding the speleogenesis of the cave from the Late Pleistocene and its human occupation. Burial and ritual activities in the cave from the Copper Age to the Middle Bronze Age have been recognized with implications on possible settlement pattern schemes with the La Sassa cave as a “persistent place” in the prehistoric human landscape. The analyses of the ceramic style in a regional framework also suggests the presence of a cultural boundary near La Sassa, which becomes highly osmotic just after the beginning of the Middle Bronze Age. The La Sassa findings provide as well implications for the seismic hazard assessment in a region inhabited by about 0.4 million people.

© 2021 The Authors. Published by Elsevier Ltd. This is an open access article under the CC BY license (<http://creativecommons.org/licenses/by/4.0/>).

* Corresponding author.

E-mail addresses: l.alessandri@rug.nl (L. Alessandri), glcardello@uniss.it (G.L. Cardello), p.a.j.attema@rug.nl (P.A.J. Attema), valerio.baiocchi@uniroma1.it (V. Baiocchi), flavio.de.angelis@uniroma2.it (F. De Angelis), silvio.delpizzo@uniparthenope.it (S. Del Pizzo), fabiana.diciaccio@uniparthenope.it (F. Di Ciaccio), angelica.fiorillo@uniroma2.it (A. Fiorillo), maurizio.gatta@uniroma2.it (M. Gatta), Monti.1614926@studenti.uniroma1.it (F. Monti), matteo.onori@uniroma1.it (M. Onori), rolfo@uniroma2.it (M.F. Rolfo), marco.romboni@uniroma2.it (M. Romboni), gianluca.sottili@uniroma1.it (G. Sottili), salvatore.troisi@uniparthenope.it (S. Troisi).

¹ These authors contributed equally to this work.

1. Introduction

The Late Pleistocene – Anthropocene transition is one of the most intriguing time ranges that allow to understand the human dispersal and cultural evolution (Fukasawa and Akasaka, 2019; Rick and Sandweiss, 2020; Smith et al., 2019; Stephens et al., 2019). A process that occurred during geological times through thousands of years and that thus had interacted with changing landscapes (e.g., Allen et al., 2000; Gatta et al., 2019; van Gorp and Sevink, 2019), that are affected by tectonic and volcanic activity, sea-level and

climate changes (e.g., the Apennines; Marra et al., 2020, 2021). In such changing context, caves are one of the most conservative environments, where archaeological, anthropological, climatic and tectonic data can be well-preserved. Their study allows the understanding of the interplay between geological processes and human use of the natural and persistent habitats in an ecosystem such as that around the cave. Today, the Apennines are a densely inhabited and seismically active mountain belt (Fig. 1) (Frepoli et al., 2017; Stucchi et al., 2004), where its axial part in Central Italy recorded earthquakes that reached magnitude up to ~ Mw 7.2, and bear evidence of neotectonics (Galadini and Galli, 2000; Galli, 2020; Roberts and Michetti, 2004; Schlagenhauf et al., 2011). By contrast, near the coast of *Latium*, despite the reports on some historical earthquakes, like the 1170 CE Ceccano Earthquake (Mw 5.5; Fig. 1) (Locati et al., 2021; Rovida et al., 2020), and the occurrence of large Quaternary fault systems, little is known about the seismogenic structures capable of destructive earthquakes (Basili et al., 2008; Faure Walker et al., 2020). At the edge of the coastal Pontina Plain and within the Volsci Range (VR), the southwestern and most internal mountain chain of the central Apennines, Quaternary monogenetic volcanic centres emplaced between ca. 800 and 350 ka are aligned with Quaternary fault zones that facilitated fast magma ascent (Cardello et al., 2020). A few tens of kilometres offshore in the Tyrrhenian Sea, Middle Pleistocene faults were recognized associated with submarine volcanoes (Cuffaro et al., 2016). Despite the well-recognized Pleistocene regional uplift and tectonic evolution affecting the southern Apennines and Tyrrhenian Basin (Bordoni and Valensise, 1999; Curzi et al., 2020), tectonic stability along the Tyrrhenian Sea coast comprised between Anzio and Gaeta during middle-Late Pleistocene has been hypothesized (Castagnino Berlinghieri et al., 2020; Ferranti et al., 2006), as opposed to a multi-phased tectonic uplift affecting the coast north of Anzio (Karner et al., 2001; Marra et al., 2016, 2019a).

However, recent work (Marra et al., 2019b, 2020) suggested that differential uplift affected the coastal ridge between Anzio and Circeo promontories (Fig. 1), coeval with subsidence of the inner sector of the Pontina Plain ("Pontina Graben", Sevink et al., 2020) during the last 250 ka. The uplift rate, its precise timing and areal extension are still the subject of debate, while a total differential uplift in the order of 30 m is documented by terraces elevation (Marra et al., 2020, and ref. Therein).

Despite the occurrence of well-known paleontological and archaeological records in the area (Alessandri, 2013; Gatta et al., 2019), no direct neotectonic evidence was either reported from the speleological exploration of the VR (Agostini and Forti, 1982). A few tens of kilometres away, some caves of the more north-eastern ranges of the central Apennines, provided evidence of co-seismic activity (Di Domenica and Pizzi, 2017; Ferranti et al., 2015; Forti and Postpischl, 1984; Pace et al., 2020; Postpischl et al., 1991).

In this work, we report on neotectonics in the Central Apennines constrained by geological, paleontological and archaeological evidence at La Sassa cave (Sonnino, about 100 km southeast of Rome, Fig. 1), by providing a methodological example for geo-archaeological exploration in caves. The cave was first investigated in 2014 during a survey of the natural caves in the Ausoni Mounts (Alessandri et al., 2020; Alessandri and Rolfo, 2015), which constitute the central mountain group of the Volsci Range. Since 2016, four archaeological campaigns were carried out at La Sassa. In the cave, between 2016 and 2019, a rich stratigraphic sequence, ranging from Late Pleistocene to the Second World War, when the cave was used by the Sonnino inhabitants as a shelter, was discovered and investigated. Our finds, constrained by a set of sixteen ^{14}C ages and numerous archaeological time markers, show that the cave was used in the Late Pleistocene (32,930–30,674 calBC) as hyena den and bear winter shelter. Much later, during the

Copper Age (CA; ca 3400–2000 calBC) and the Bronze Age (ca 1900–1400 calBC), as a burial place. The upper portion of the archaeological deposit in rooms 1, 2 and 3 also shows some medieval and renaissance activities which partially reworked the Bronze Age layers. Starting from 2018, an almost complete 3D model of the cave merged with the outside ground surface was obtained to support the archaeological interpretations and the multiscale geological survey performed in the surroundings. As later discussed, this work bears implication for seismic hazard assessment in the region, setting the ground for further investigation in the Quaternary and Holocene/Anthropocene units and other caves of the region and elsewhere. This work aims also at bridging the current interest in the Anthropocene with landscape evolution before and after the impact of human use of a cave began as it well shows the interplay between geological processes and human use of the natural and persistent habitats. A speleogenic comparison with karst systems worldwide is presented in the discussion as well as a contextualization of the archaeological finds in the frame of the regional landscape evolution.

2. Regional setting

2.1. The geological and palaeontological setting

The La Sassa cave occurs (Fig. 1) in the Quaternary lithified breccia deposited in a valley of the Volsci Range (VR), the most extensive mountain range of the Central Apennines (Carminati et al., 2012; Cardello and Doglioni, 2015; Cardello et al., 2021). The VR is mostly composed of carbonate rocks and it comprises three major mountain groups, Lepini, Ausoni and Aurunci Mounts, located between the Colli Albani Volcanic District (0.6–0.04 Ma) to the northwest and the Roccamonfina volcano (0.5–0.1 Ma) to the southeast (Marra et al., 2021 and references therein). In the Ausoni Mounts, Cretaceous shallow-water carbonates crop out while discontinuous Cenozoic temperate ramp deposits occur in the Latin Valley (Centamore et al., 2007; Consorti et al., 2017). At the top of the carbonate succession, middle to upper Miocene syn-orogenic siliciclastic rocks and marls are locally found at the footwall of the thrustured carbonate units (Angelucci, 1966; Cosentino et al., 2002; Cardello et al., 2021). During the Messinian salinity crisis, between 5.96 e 5.33 Ma, the area was exposed to fluvial erosion followed by the deposition of early Pliocene sandy gravels ranging between 5.33 and 4 Ma (Centamore et al., 2010). Near our study area, according to the averaged uplift history of the nearby Simbruini Mounts (Fig. 1; Delchiaro et al., 2020), which are just north of VR, about 2.4 Myr of Quaternary uplift are recorded. In particular, from 2.4 to 1.65 Ma, the baselevel fall rate constantly reached the highest value of about 690 m Ma^{-1} . Then, from 1.65 Ma to 0.75 Ma it temporarily decreases at around 1.3 Ma . As at 0.75 Ma, the baselevel fall rate reaches its minimum of about 370 m Ma^{-1} , the uplift rate raised again until the present day with a value of about 660 m Ma^{-1} . From the occurrence of deposits of early Pliocene deposits at the bottom of the valleys (Centamore et al., 2010), also our study area experienced regional Quaternary uplift from at least the Middle Pliocene. After emersion, erosional terraces were displaced by tectonics that brought them to different elevations (Centamore et al., 2007). During the late Pliocene, the VR was uplifted together with the rest of the Apennines, while the Pontina Plain was invaded by seawater (Boni et al., 1980). In the VR, from the Early Pleistocene, crustal uplift was accompanied by normal faulting, which generated a horst-and-graben structure with fault-bounded marine to continental basins towards the inland. The oldest Quaternary deposits recorded in the hinterland, suggest that atop the downthrown normal fault blocks, lacustrine to fluvial sedimentary conditions occurred, bearing geomorphological

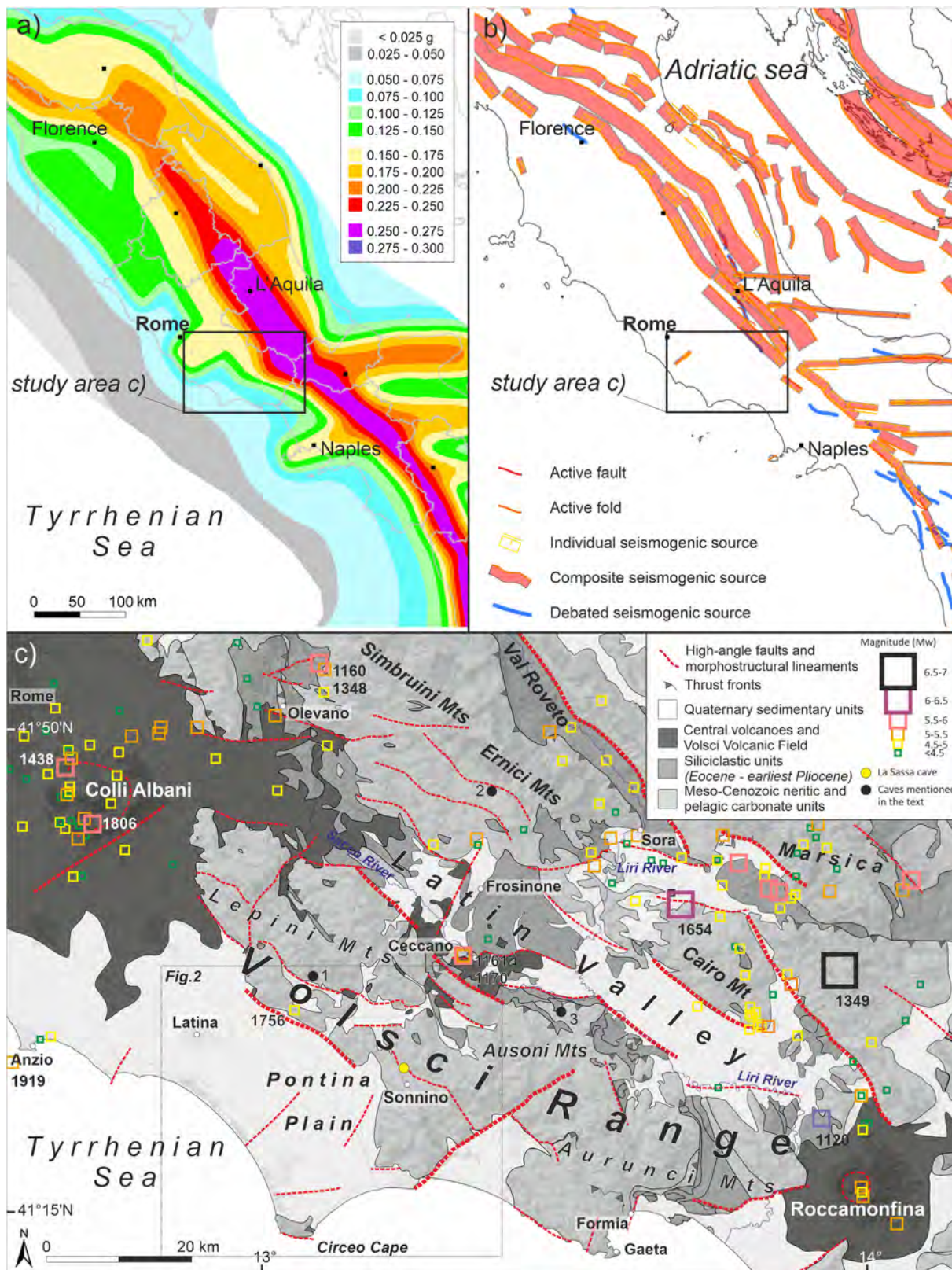


Fig. 1. Geological setting. (a) Seismic hazard map of central Italy (Stucchi et al., 2004). (b) Individual seismogenic sources of central Italy (Basili et al., 2008). (c) Reviewed sketch geological map of the Volsci Range (modified after Cardello et al., 2021) with the location of La Sassa cave (yellow dot, coordinates of the entrance: WGS84, 41°25'30"N, 13°14'11"E), other caves mentioned in the text (1, Vittorio Vecchi; 2, Regina Margherita; 3, Pastena) and the historical earthquakes (Rovida et al., 2020). (For interpretation of the references to colour in this figure legend, the reader is referred to the Web version of this article.)

evidence of ongoing tectonics (Centamore et al., 2010). Until the Middle Pleistocene, volcanic terrains comprise distal tephra from nearby potassic volcanoes recognized within continental successions in the Latin Valley and in the Pontina Plain (Alessandri, 2019; Centamore et al., 2010; Sevink et al., 2020). In the VR intermontane depressions of the Lepini and Ausoni Mountains and the Latin Valley are punctuated by volcanic occurrences of Pleistocene age also from local eruptive centres (Fig. 1) (Cardello et al., 2020; Marra et al., 2021). Notably, lower to upper Pleistocene slope, river and lacustrine deposits are preserved within depressions determined by high-angle NW-, ENE- and (N)NE-striking normal faults that dissected the inherited fold-and-thrust fabric, influencing the distribution of 1) Quaternary deposits; 2) karst form and 3) the fluid circulation. Quaternary slope deposits occur as breccia formed after the dismantling of mountain chains during glacial periods (Blanc and Segre, 1953; Hughes and Woodward, 2008; Petronio et al., 2007). In the nearby, Circeo Mt continental reddish breccia occurs at the seaside. In the VR, similar rocks occur at an altitude comprised between about 150 and 50 m. While in the Circeo Mount they were attributed to the last ice age (between 55 and 33 ka, Blanc and Segre, 1953), in the VR area, they are still undetermined. After their deposition, these breccia units were karstified and the caves were occupied.

During the Late Pleistocene, the Pontina Plain (also known as Pontine swamps or plain in the Archaeological literature) was characterized by a varied landscape. Its high biodiversity and ecology turned it into refugial environment during the rapid and severe climatic fluctuations of the Marine Isotope Stage (MIS) 3 and 2 (57–11.7 ka BP) (Allen et al., 2000; Gatta et al., 2019). It consisted of at least three coexisting temperate ecosystems including humid and swampy coastlines, a vast steppe-grassland plain with numerous streams and extensive Mediterranean woods populated by a broad spectrum of large and small vertebrates, reptiles and amphibians (Gatta et al., 2016, 2019).

Archaeological and paleontological sites in the Pontina Plain (among others Canale delle Acque Alte and Cava Muracci; Blanc, 1935; Farina, 2011; Gatta et al., 2019; Gatta and Rolfo, 2017) and the many caves of Mount Circeo (e.g., Grotta Guattari, Grotta del Fossellone, Grotta Breuil; Blanc, 1954; Stiner, 1991) have yielded important data on human presence, distribution of fauna and climate variability during the MIS 3–2 transition covering the time frame from 35 to 33 ka. After the last Holocene transgression (6ka BP; van Gorp et al., 2020), marine terraces underwent soil formation and created a gully landscape in the Fondi plain and in the south-eastern Pontina Plain (Fig. 2) (see also van Gorp and Sevink, 2019).

At around 1900 BCE (van Gorp and Sevink, 2019), the dune ridges closed the south-eastern marine lagoons at the foot of the Volsci Range near present-day Terracina, forming a lacustrine to marshy environment. The infilling lacustrine to marsh deposits are thicker where the effects of subsidence were enhanced (i.e., after the 1919–29 reclamation of the Pontine swamps; Serva and Brunamonte, 2007). Nowadays, the main VR hydrogeologic unit has a piezometric head below 125 m above sea level (Boni et al., 1980), making the whole area still subjected to karst. Similar to what observed elsewhere in the Central Apennines (e.g., Barberio et al., 2021), springs are associated to mixing deep fluids along the main normal faults.

As shown in Fig. 1, the distribution of historical earthquakes in the region is mostly clustering far from our study area (i.e., in the Colli Albani, and Sora-Marsica; Fig. 1). However, earthquakes also cluster at the edge of the Latin Valley graben, while in the Pontina Plain their occurrence was sporadically recorded near Anzio (also offshore) and along the foot of the Volsci Range (Fig. 1) (Sezze earthquake 1756, Mw 4.4; Rovida et al., 2020), where a major

WNW-striking normal fault bounds the plain.

Being at the edge of the more seismic Apennine backbone (Frepoli et al., 2017; Stucchi et al., 2004), a large part of the study area was traditionally considered inactive because of the lack of volcanic and seismic historical events. For this reason, this area was chosen in the 1950s as an ideal setting to install two nuclear power plants. Unexpectedly, two seismic sequences in 2011 and 2012 shook the Pontina Plain with earthquakes of moderate magnitude ($M_w \leq 3.8$; <http://iside.rm.ingv.it>), demonstrating that tectonic faulting may suddenly occur. On <http://terremoti.ingv.it/search> the distribution of recent earthquakes is kept up-to-date.

2.2. The archaeological setting

Despite systematic archaeological research (Fig. 2a), almost all evidence for the Copper Age (CA) and Bronze Age human activity comes from either un-systematic surveys or has been found by chance. Therefore, the CA and the Early Bronze Age (EBA) landscape is poorly known. The few CA pottery sherds in the area (Carboni, 2002, 2019 and references therein) (Fig. 2b) point to a material culture influenced by the southern Italian facies. The EBA has been recently targeted by the Avellino Project, which aimed at reconstructing the landscape and human occupation around the time of the Avellino Eruption (around 1900 BCE, Alessandri et al., 2019; Attema et al., 2019; van Gorp et al., 2020, Sevink et al., 2020). Since only few EBA potsherds have been retrieved during systematic and targeted surveys, it is likely that the Pontina Plain and the VR in the EBA were very scarcely populated (Fig. 2c). A different picture emerges from the beginning of MBA (Fig. 2d), when the north-western portion of the Ausoni Mountains and the coastal strip were more densely occupied (Alessandri, 2013 and references therein). At the beginning of MBA (subphases 1–2), the material culture of the Tyrrhenian side of the peninsula was characterised by two widespread ceramic styles: the Grotta Nuova facies, in the central part, and the Protoappenninico facies in the southern part (for a definition of the facies see Damiani, 1995 and Cocchi Genick, 2002). Already in 1995, Cocchi Genick (1995) and Damiani (1995) placed their boundary in the Pontina Plain (Fig. 2d, upper right).

Using natural caves as places for burial are typical of CA, EBA and MBA. In the surroundings of the La Sassa cave, a good example is the Vittorio Vecchi cave (Fig. 2), where the disarticulated human remains of more than 40 people were recovered together with a considerable number of potsherds dated from CA to MBA (Guidi and Rosini, 2019). According to the authors, the potsherds belonging to the MBA1A subphase resemble the Grotta Nuova facies, while in the next subphase (MBA1B) some typical stylistic traits of the Protoappenninico facies are also present. As supported by recent investigations, also the La Sassa cave was used for human burial between the Copper Age and the Middle Bronze Age.

3. Material and methods

3.1. The geological methods

In the La Sassa cave, an additional geological-structural survey of the rocky substrate was carried out, integrating the previous work (Accordi et al., 1966). Field work aimed to re-define the general stratigraphic and structural architecture of the La Sassa area and identifying the main structural trends of the area. To this end, as shown in Fig. 3, faults and fractures have been described at key localities. Also, the morpho-structural interpretation is based on both field checks and the analysis of the orientation of river and valley segments and relieves characterized by break-in-slopes and near-surface fault traces cutting through Cretaceous carbonate and Quaternary deposits. In these units, the analysis of break-in-slopes

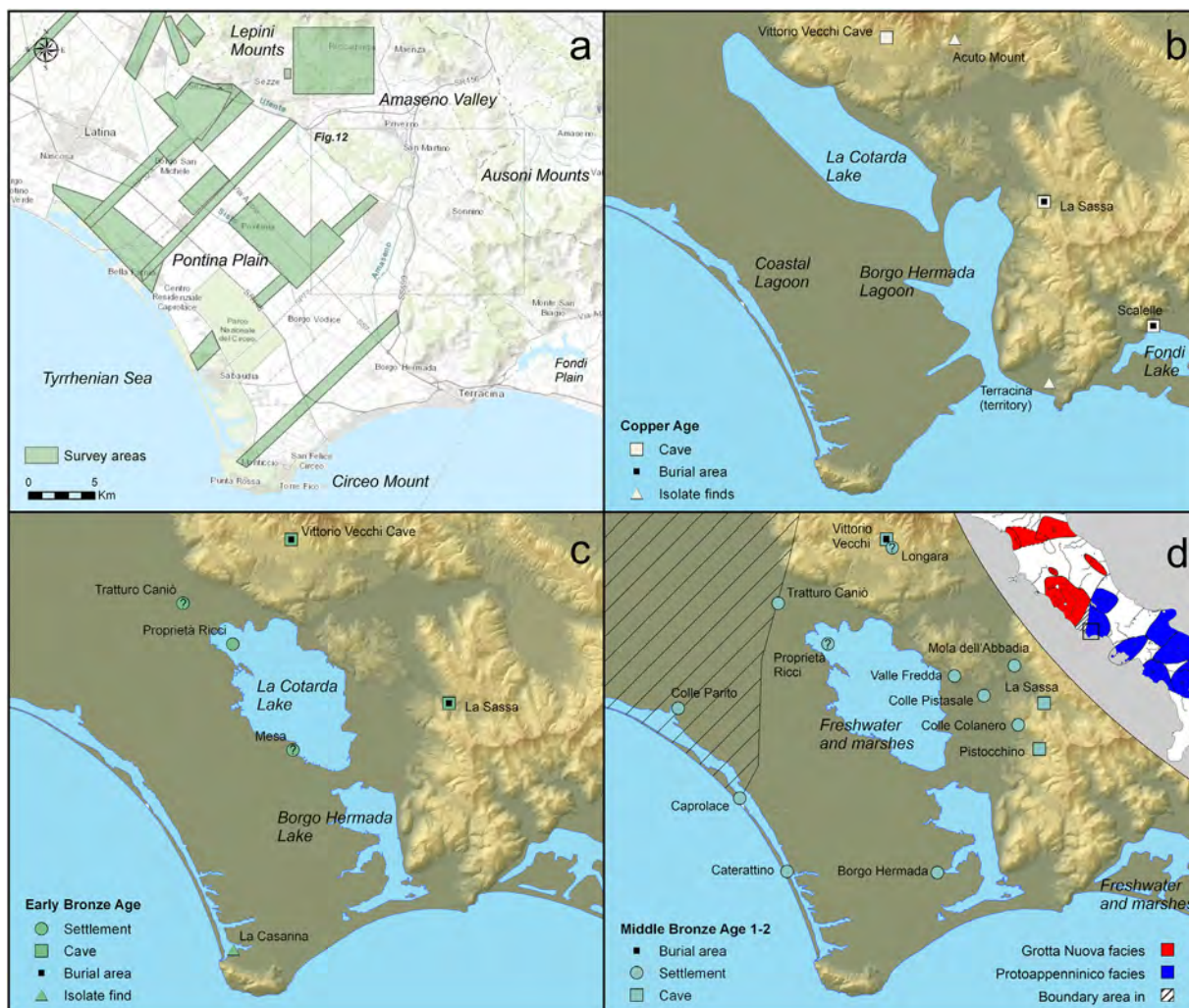


Fig. 2. Archaeological setting. (a) Areas in which archaeological surveys have been carried out. Background from Esri, DeLorme, HERE, TomTom, Intermap, increment P Corp., GEBCO, USGS, FAO, NPS, NRCAN, GeoBase, IGN, Kadaster NL, Ordnance Survey, Esri Japan, METI, Esri China (Hong Kong), Swisstopo, MapmyIndia, and the GIS User Community. (b, c, d) Copper Age (CA), Early Bronze Age (EBA) and Middle Bronze Age (MBA 1–2) evidence around La Sassa cave. In the top right corner of (d), the areas characterised by Grotta Nuova and Protoapenninico facies, modified after Damiani (1995). CA sites from Carboni (2019), 2002; EBA and MBA sites from Alessandri (2013). Background DEM from TINITALY/01 (Tarquini et al., 2007). Reconstruction of the lakes and lagoons modified after Alessandri (2013), van Gorp and Sevink (2019) and van Gorp et al. (2020).

>20% recognized on the LiDAR Digital Terrain Model (e.g. Cardello et al., 2020) allowed tracing morphostructural lineaments crossing and bounding the Cretaceous carbonate relieves and the Quaternary units. The collected geological data support inferences on the sub-surface deeper geometry of faults schematically represented in the cross-sections and in a block diagram, which allow to roughly determine the lateral extension of faults (fault length) and their related offset. Structural data (e.g., faults, fractures, bedding) were measured in the field and plotted by using TectonicsFP (Ortner et al., 2002).

3.2. The archaeological methods

During the four archaeological campaigns, the cave was subdivided into rooms and soundings were carried out in most of them. Both rooms and soundings were named by alphanumeric code. All the finds and layers described in this paper were carefully recorded in a local coordinate system and then transformed into EPSG (European Petroleum Survey Group): 32,633, which corresponds to the World Geodetic System 84, Universal Transverse of Mercator projection, zone 33 N. The finds received a unique

number and are now stored at the Laboratory of Prehistory at the University of Rome Tor Vergata along with all the original datasets, recorded in a digital database. The relative chronology of contexts was assessed by ceramic typo-chronological parallels; the absolute chronology by radiocarbon date on human and animal bone. The demographic parameters were estimated according to several consolidated methods based on the available skeletal districts (Bruzek, 2002; Houdaille et al., 1972; İşcan, 1985; Lovejoy et al., 1985; Meindl et al., 1985; Ubelaker, 1989).

The walking-time distances from the settlements to the necropoleis were calculated using the path-distance function in ESRI ArcGis. The movements were simulated following the so-called Naismith (1892) rule with the Langmuir (1984) correction.

Excavation and study permits were received yearly from the Soprintendenza Archeologia, Belle Arti e Paesaggio per le Province di Frosinone, Latina e Rieti (2016: n. 4888 Class 34 31. C7/328.1; 2017: n. 9559 Class 34.31.07/74; 2018: n. 0013261-P Class 34.31.07/7, January 11, 2018; 2019: n. 0016086-P Class 34.31.07/7, January 11, 2018).

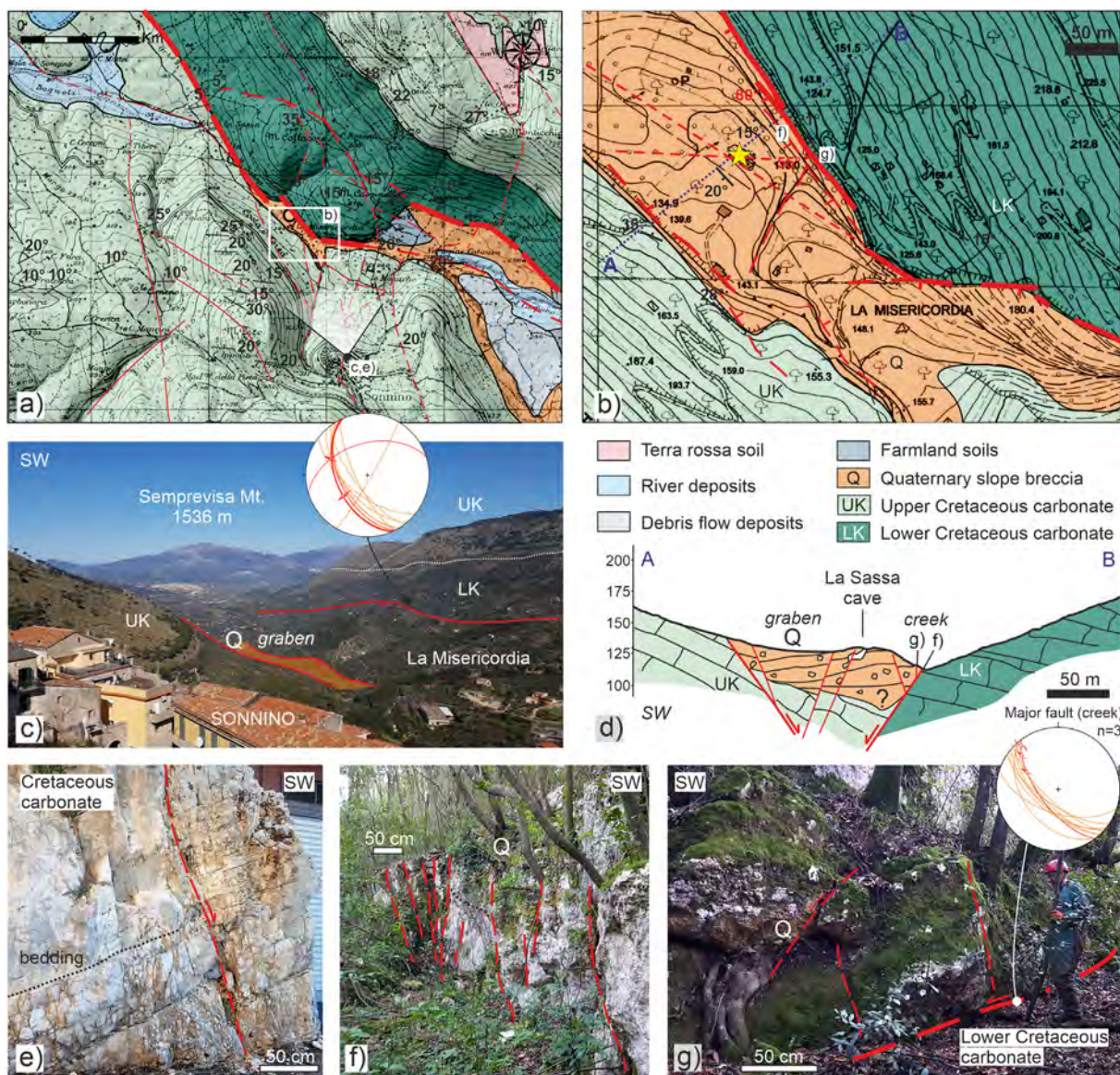


Fig. 3. Geology of the surroundings of the La Sassa cave. (a) Geological map modified after (Accordi et al., 1966) and <https://sit.provincia.latina.it/>. (b) Structural detailed map of the surroundings of the La Sassa cave showing cross-section AB (blue dashed line) and location of the La Sassa valley and cave (yellow star). (c) Panoramic view of the La Sassa valley from Sonnino village with stereonet of lower hemisphere projection of fractures (orange) and faults with slickenfibers (red) measured on the Carbonate ridge to the north (Le Camminate locality, WGS84, 41°26'4"N, 13°14'39"E). (d) Geological cross-section AB of the graben with the location of geological evidence below. The cross-section is supported by field data and it has been drawn along the mean direction of transport towards the northeast during the Apennine collision. (e) NW-striking fractured carbonates at Sonnino. (f) North-west striking fractured Quaternary breccia and (g) fault contact with Cretaceous carbonates in the La Sassa at the northern edge of the graben (WGS84, 41°23'32"N, 13°14'11"E) with stereonet of lower hemisphere projection of fractures (orange) in the breccia (f) and faults with slickenfibers (red) measured at (g). (For interpretation of the references to colour in this figure legend, the reader is referred to the Web version of this article.)

3.3. Three-dimensional internal and external modelling with geomatic techniques

The 3D model of the cave is the result of two distinct photogrammetric surveys performed during the excavations. Different cameras and light dispositions were used. Due to the narrow environment, the most complex and inaccessible areas (e.g., Branch and Room RA) were surveyed using the camera and the light of a smartphone Xiaomi Mi 9. The remainder of the cave was modelled by processing images extracted from videos recorded by a Nikon D800E camera with a fisheye lens, following a procedure already employed successfully in the survey of other underground environments (Troisi et al., 2017).

The photogrammetric model was georeferenced and scaled

using three Ground Control Points (GCPs), previously obtained by a Global Navigation Satellite System (GNSS) survey. Double frequency Topcon Legacy-e receivers were employed to acquire the points, which were further differentiated according to the permanent stations of the Lazio Region, obtaining almost 25 mm horizontal estimated accuracy and 40 mm estimated vertical accuracy. Since these points could only be placed in the external part of the cave, further constraints were necessary to minimise the deformations of the most inner parts. For this reason, some targets were placed on the internal walls and their relative distances were measured.

Unfortunately, at branch RA, these constraints were not applied due to the very narrow space. Consequently, the survey was conducted about 1 year after the first photogrammetric survey. To

update the 3D model including the new Room RA, a 3D-Helmert transformation was carried out taking the first survey as reference. The alignment was then refined using the ICP technique, providing a Root-Mean-Square Error (RMSE) of 12 mm. The complete 3D model was then linked to the Rete Dinamica Nazionale 2008 (RDN, 2008; EPSG: 7792).

Outside, a drone photogrammetry survey was performed with a quadcopter DJI Phantom 4 equipped with its standard camera to obtain a high-density 3D model of the terrain surrounding the cave. The flight planning was conducted to assure a 15 mm Ground Sample Distance on the ground. During the flight the drone acquired 343 nadir images with a geometric resolution of 5472×3648 pixels, to cover a zone of 30,000 m². At the end of the processing, a Digital Surface Model (DSM) was obtained on the basis of a dense point cloud of about 25 million points. To correctly orient the model, a further ground survey was carried out to estimate the coordinates of ten GCPs using the same GNSS receiver with the same accuracy. The obtained result was referred as well to the EPSG: 7792 reference system, with an RMSE of 30 mm on the GCPs and an RMSE of 90 mm on the Check Points (CPs).

3.4. Radiocarbon dating

The human and fauna bones were sampled according to their stratigraphical position. Two samples were analyzed at the CIO (Centre for Isotope Research, code GrA) of the University of Groningen (methodology details in [Dee et al., 2019](#); [Mook and Streurman, 1983](#)). Eleven samples were analyzed at the CEDAD (Centro di Datazione e Diagnostica, code LTL) of the University of Salento (methodology details in [Calcagnile et al., 2019](#)). Three more samples were analyzed at the ORAU (Oxford Radiocarbon Accelerator Unit, code OxA) by using the ultrafiltration protocol AF (see details in [Brock et al., 2010](#); [Higham et al., 2006](#)). Finally, all the radiocarbon dates were calibrated with OxCAL4.3 using the IntCal13 curve ([Reimer et al., 2013](#)).

4. Results

4.1. Large-scale geological evidence

The mesoscopic geological setting of the area surrounding the La Sassa cave is dominated by several kilometres long normal faults ([Fig. 3](#)) that cross-cut Lower to Upper Cretaceous carbonate units. Overall, the Cretaceous carbonate groups have a total minimum thickness of about 1 km, being the Upper Cretaceous group characterized by channelized rudist fragments-rich limestones, while the Lower Cretaceous group is richer in dolomites. Both Cretaceous carbonate units and Quaternary breccia are affected by linear karstic incisions, which often occur at fault zones rich in fractures (both in the footwall and in the hanging wall of major faults). In the area, occasionally speleothemes were found associated with areas with higher fracture density. As reported on the map of [Fig. 3](#), the valleys are infilled by Pleistocene to Holocene deposits. By comparing the orientation of our structural data with these linear forms, retrieved from the combined analysis of LIDAR field and field data along the most evident fault traces (see section 3.1), we distinguished between major (thick dashed lines) and minor fault lineaments (thin dashed lines) in the area ([Fig. 3](#)). Overall, we observe a 10–12 km long segmented fault-arrangement disposed along a dominant NW-striking fault set, being the longest segment up to 3–4 km each.

Nearby NE-striking faults can reach comparable lengths. Minor faults are NNW- to NNE-striking and are of limited lateral extent (i.e., 1.3 km on average). In places (e.g., at La Misericordia [Fig. 3b](#)), the NW-striking segments are connected and locally crosscut by

ENE-to WNW-striking cross-faults with oblique kinematics. These fault sets occur as high-angle faults with dip ranges between 50° and 85°. The cumulative fault offset associated with this extensional system along the main NW-striking system is in the order of about 0.8–1 km distributed on about 2–3 major fault branches down-stepping towards the SW. In this frame, the La Sassa valley has been recognized as a graben bounded by antithetic normal faults clearly dissecting at least a 0.5 km thick pile of upper Cretaceous carbonate that is locally well-fractured near the major graben-bounding faults ([Fig. 3](#)). The major fault bounding the north-western edge of the valley is an oblique normal fault with a left lateral component ([Fig. S1](#)). The morphology of this localities is characterized by vertical shafts and sinkholes (i.e., Voragine Catausa; La Sassa). Their elongation corresponds to a well-incised valley that connects two different basins placed northwest and northeast of Sonnino, La Sassa valley being the northwesternmost ([Fig. 3](#)). Close to the north-eastern bounding fault, the breccia occurring at the top are affected by dominant near-vertical NW- and ENE-striking fractures that overall run parallel to the master fault. At La Sassa locality, the bedding of the deposits, that partially fill the valley is constituted by a succession of Quaternary breccia deposits that gently dips towards the SW. The morphological evidence suggests that the Quaternary slope breccia deposits are topped by an erosive surface generating a fluvial terrace (e.g., north and east of Sonnino; [Fig. 3](#)). Supported by a more detailed field survey and geomorphic analysis on the LiDAR dataset, we report that the NW-striking fractures affecting the breccia in the surroundings of the La Sassa cave ([Fig. S1](#)) are associated with NW-striking topographic breaks of the slopes with jumps in the elevation in the order of a few meters ([Fig. 3](#)). These fractured zones bound cultivated depressions that are some meters across, and are filled by Quaternary to more recent soil deposits.

4.2. Geology of the La Sassa cave

Underground fieldwork allowed to recognize that the bedrock mostly crops out on the roof of the north-western part of the cave ([Fig. 4](#)), where it is constituted of clast-supported and cemented continental breccia with rare soil-derived matrix arranged in irregular layers that dip about 15–30° to the southwest ([Fig. 5](#)). The clasts contained within represent the Cretaceous carbonates (often with rudists). On the roof, at the edge between rooms 1–2 and rooms 3–7 and in room RA, dm-scale stalactites and sails of calcite abound near areas where fractures are more abundant. On the floor, a collapse-derived deposit of fallen blocks of breccia bedrock and more recent soil occur at the present-day entrance, in the NE portion of Room 1, between the latter and Room 3, the Branch and Room RA. On the fallen blocks limiting the southwestern walls of the rooms of the cave, fossil stalagmites and coalescences of columns occur. The fossil concretions bound the internal terraces that constitute 2–4 m large and some decimetric to centimetric thick ponds. Within these depressions, soils rich in archaeological materials are preserved. Active concretioning is limited to the deepest and southwesternmost part of the cave.

Two sets of faults with faint slickenlines were found at the old entry, indicating NE-striking dip-slip and (W)NW-striking right-lateral faults ([Fig. 5c](#)). On the south-western wall of Room 1 normal to oblique right-lateral kinematics were found. Overall, the structural analysis of the fractures accompanying faults and concretioned lineaments of the cave allows identifying three major morpho-structural lineaments representative of NW-, E (NE)- and (N)NE-striking fault sets ([Fig. 5d](#)). The fault sets recognized in the cave can be compared with the faults and fracture recognized outside the cave ([Fig. S1](#)). No clear cross-cutting relationships could be established between the different fault sets.

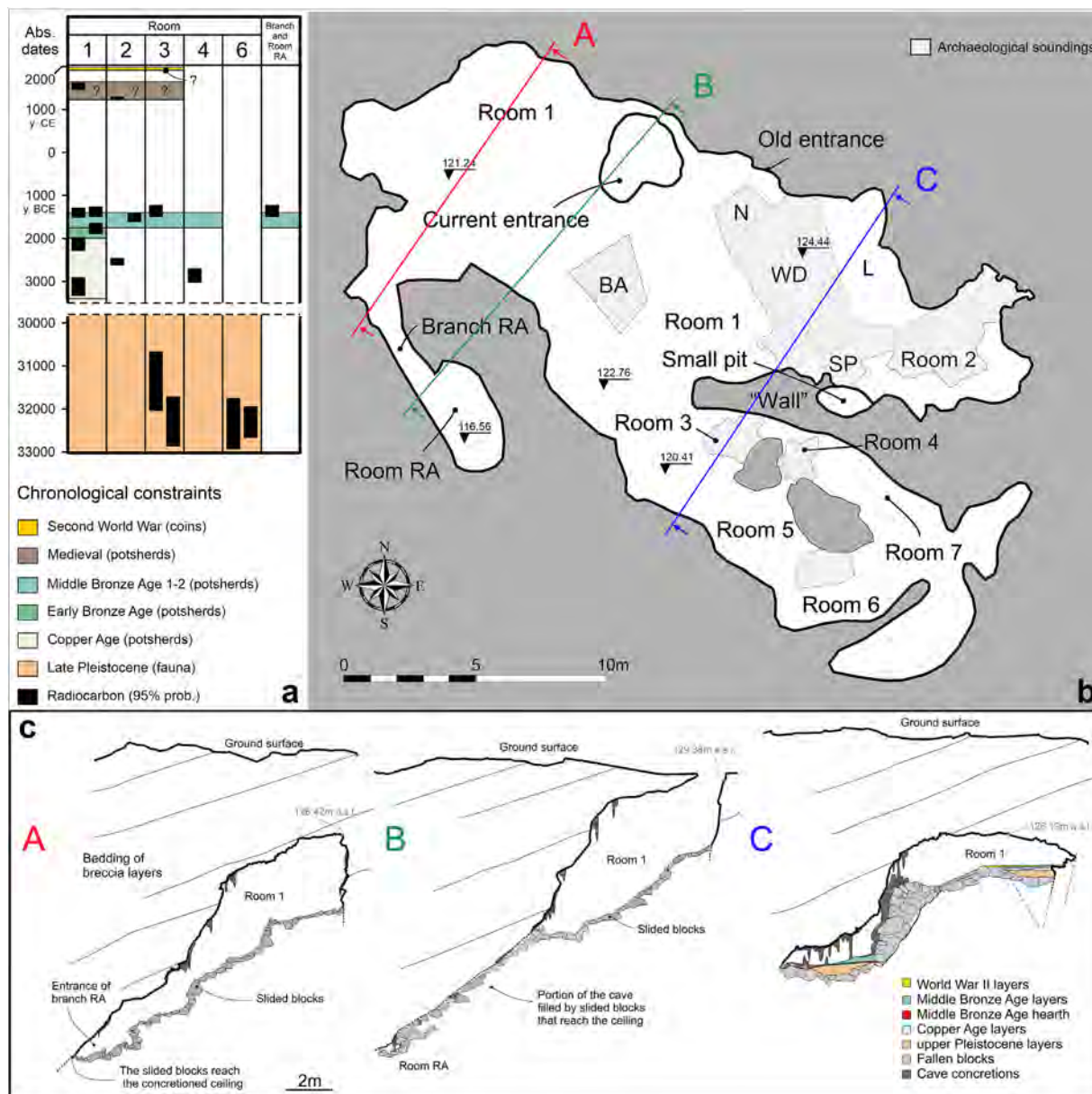


Fig. 4. Chronology and map of the archaeological soundings at La Sassa cave. Different portions of the cave have been labelled rooms and branches and named with alphanumeric codes. (a) Chronological (relative) phases and radiocarbon (absolute) dates. (b) Schematic map of the La Sassa Cave with the archaeological soundings and the cross-sections A, B and C decorated with speleothems, concretions, collapsed blocks and debris. The “wall” made of rocks and concretions between rooms 1–2 and 3–7 is also indicated. The cross-sections of the cave have been extracted from the photogrammetric 3D model. Structural data projection is shown in Fig. 5.

With regards to the structure within the cave, the roof of Room 1 is flat in the inner part while it abruptly dips towards the southwest of about 75°. There, near the most intensely fractured zones, concretions occur on the roof as well as on the floor. In Room 1, ENE- and WNW-striking concretion lineaments occur, while the NW- and (N)NE-striking sets bound the longest edges of the cave. Of note, about 1.5 m across large loose blocks of breccia occur at the entrance between room 1 and 3. Also, the ENE-striking set runs along a concreted fallen-rock assemblage, dividing Room 1 from rooms 3–7. Approaching this wall, fractures are healed by sail-type concretions that get coalescent and share the same orientation as the wall.

This clearly marks the limit between the area with a few or free of concretions (northeastern side of Room 1) and the rooms rich in concretions (rooms 3–7) (Fig. 5, S1). As the ENE-striking lineament

is locally interrupted by NNE-striking and NE-striking concretions, fractures with different orientations occur.

Between rooms 1 and 3, a column is crosscut by a SW dipping fracture, which is partially healed by later speleothems (smaller size columns) (Fig. 5f). Three geological cross-sections obtained from the 3D model of the cave allow quantifying the observed height offset between the flat parts of the roof of Room 1 and Room 3, which is 4.75 m high. This topographic step is accompanied by blocks and concretions that, depending on the sector of the cave, together with soil of different ages healed or partially sealed the break in offsets in the cave. Worthy of note, between Room 3 and Room RA, the vertical offset is about 3.64 m, where a massive concreted collapse breccia is almost wholly sealing the scarp. At Branch RA, a further NW-striking abrupt termination is observed to the south-west. As shown in the map (Fig. 5), minor NE-striking

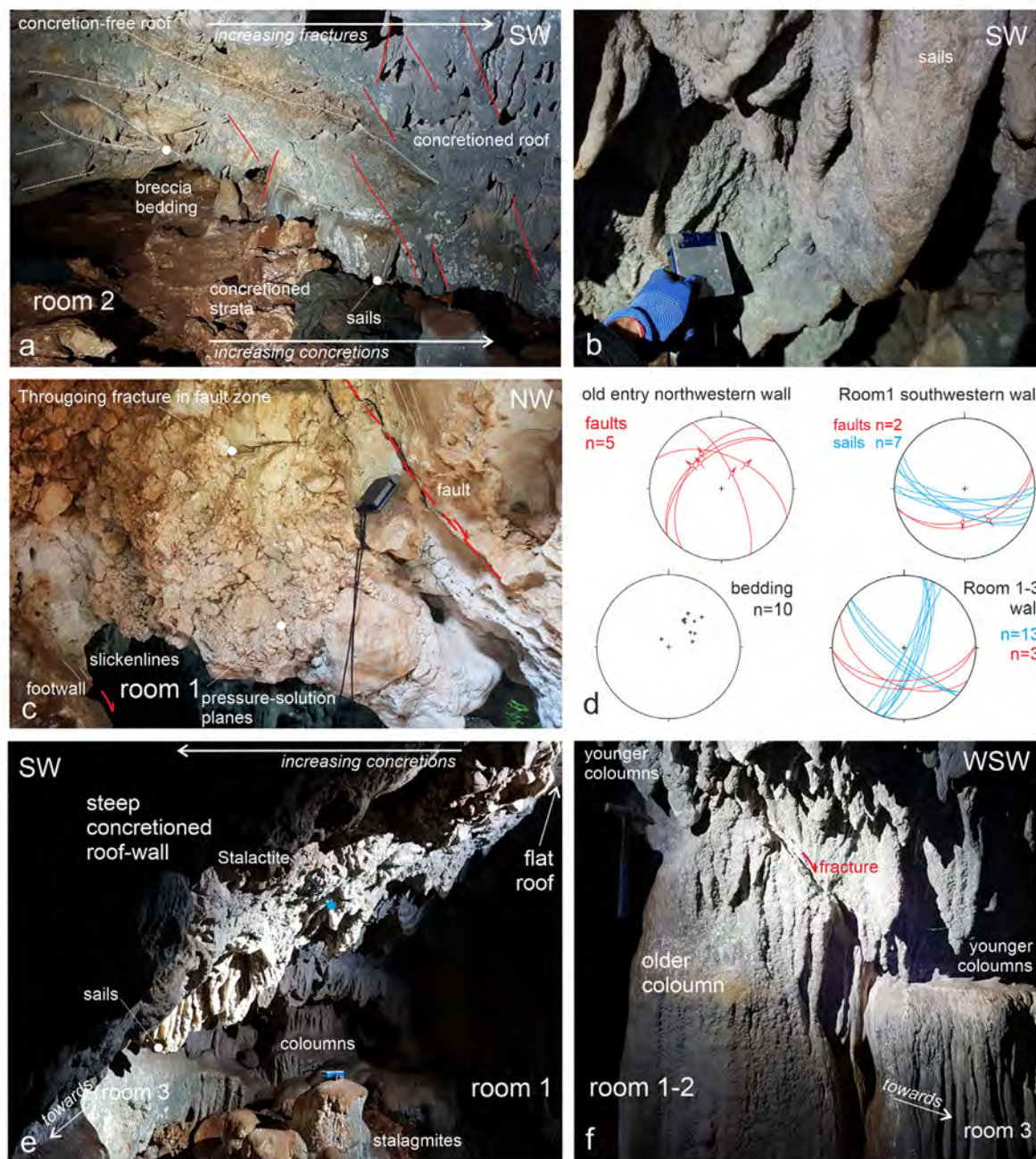


Fig. 5. Structural evidence in the La Sassa cave. (a) Room 2, increase of fractures and sealing concretions towards the SW. (b) Detail of NW striking calcitic elonged sail concretions. (c) Old entry of Room 1, fault core breccia within NE striking fault. (d) Lower hemisphere stereo-plot projections of key fractured and concreted areas. SW wall of Room 1 with increasing concretions towards the fault wall. (f) Detail of the syn-tectonic column concretion characterised by through-going fracture within a column later healed by younger columns.

lineaments occur between different rooms and at the room edges.

4.3. The late pleistocene finds and chronological constraints

Variably thick upper Pleistocene layers have been identified in Rooms 1, 2, 3 and 6. These yielded hundreds of coprolites and almost 5000 bone remains belonging to at least 23 different faunal taxa. Bone remains with gnawing traces by at least one large carnivore and hyena coprolites were found in primary position in Rooms 1 and 2. Faunal remains from Room 3 were collected from a

partially concreted layer sealing the (almost) 4 m-thick deposit, composed of fallen blocks of breccia (up to 1.5 m across each) relatively free of concretions and which probably lie directly on some blocks on the cave floor. In this deposit, we found bone remains in often vertical position. In room 6 (Figs. 5 and 6), a well-preserved adult skeleton of a brown bear (*Ursus arctos*) in partial anatomical connection and a few other isolated bones belonging to a second specimen were found. Most of the bone remains were covered and partially embedded in the stratigraphic unit SU 16, a highly concreted calcitic crust 5–7 cm thick (Fig. 6). A small number



Fig. 6. The bear from Room 6. (a) The bear bones covered by concretions before the start of the excavations. (b) The radiocarbon dated right radius (LS 35). (c) A left tibia. (d) SU 16, Astragalus almost completely embedded by concretions; remains of macro and micro fauna are visible.

of bones lay on a soft brownish clay layer underneath (SU 17). As in Room 3, also in Room 6, the lower stratigraphic unit is free of concretions. No cutmarks and gnawing traces occur on the bones of the bears.

The four radiocarbon dates on hyena and bear bones from Rooms 1, 3 and 6 (Table 1) constrain these deposits between 32,930–30,674 calBC (Fig. 7b).

Table 1
Radiocarbon dates from La Sassa. Calibration done with OxCal 4.3, IntCal13.

Lab code	Sample code	Context	Sample	14C age	STD	Calibrated age (OxCal4.3, IntCal13, 95.4%)
GrA64830	LS 35	Room 6, SU 16	<i>Ursus arctos</i> , right radius	30,210	180	32,665–31,945 calBC
OxA-37283	LS 3	Room 6	<i>Ursus arctos</i> , right radius	30,220	360	32,930–31,755 calBC
OxA-37219	LS 516 ^a	Room 3	<i>Crocota crocuta</i> , mandible	30,150	350	32,862–31,722 calBC
OxA-37218	LS 516b	Room 3	<i>Crocota crocuta</i> , mandible	29,190	310	32,037–30,674 calBC
LTL19066A	LS 2993	Room 1, SU 97	Human femur	4409	45	3327–2911 calBC
LTL18164	LS 1014	Room 4, SU 25	Indeterminate, vertebra	4271	45	3019–2701 calBC
GrA64828	LS 418	Room 2, SU 19	Human femur	4000	35	2619–2462 calBC
LTL19064	LS 605	Room 1, SU 55	Human femur	3722	40	2278–1980 calBC
LTL19065A	LS 873	Room 1, SU 78	Human femur	3451	45	1888–1646 calBC
LTL18166	LS 1047	Room 2, SU 31	Ovis sp., right humerus	3205	45	1611–1406 calBC
LTL20395A	LS 2176	Area RA	Human femur	3165	40	1519–1306 calBC
LTL17395A	LS 430	Room 1, SU 9	Sus sp., right ulna	3148	45	1506–1293 calBC
LTL18165	LS 1040	Room 1, SU 26	Sus sp., radius	3112	40	1492–1266 calBC
LTL17393A	LS 425	Room 3, SU 7	Sus sp., left radius	3101	45	1492–1233 calBC
LTL18163A	LS 921	Room 2, SU 18	<i>Canis familiaris</i> , right radius	745	30	1222–1290 calAD
LTL17396A	LS 431 + LS 432	Room 1, SU 9	<i>Canis familiaris</i> , third left metatarsal and left heel	347	45	1456–1641 calAD

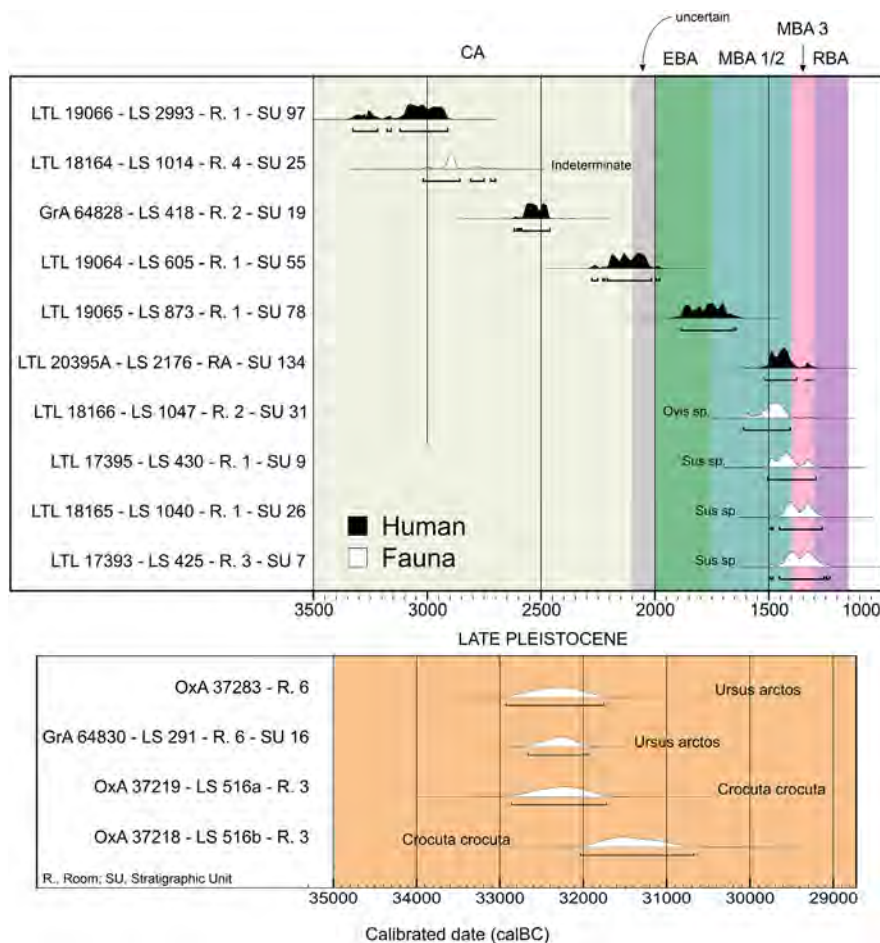


Fig. 7. The radiocarbon dates (a) Copper Age and Bronze Age. (b) Pleistocene. R., Room; RA, Room RA; SU, Stratigraphic Unit. Calibration done with OxCal 4.3, IntCal 13.

4.4. The Copper Age and Bronze Age finds and chronological constraints

In rooms 1 and 2, hundreds of disarticulated human bones were found just above the upper Pleistocene deposits. Their distribution could be due both to naturally occurring sliding and intentional reductions (Fig. 8a and c).

The osteological evaluation allows to determine a Minimum Number of Individuals of 20, including adults and at least three skeletally immature individuals. The osteological and osteometric analysis showed that adults buried in the cave were both males and females (four men and four women were osteologically identified), ranging from young (20–25 years) to senile individuals (over 50 years), showing that access to the funerary area was not restricted by age or sex. A few potsherds were found together with the human bones. However, none of them was diagnostic for time or cultural constraining, as it was not possible to reconstruct the shape of the vessels. The radiocarbon dates (Fig. 7 and Table 1) on some human femurs range from the CA to the EBA.

In Room RA, several meters away from the other disarticulated bones, an infant (1–2 years old) was recovered and radiocarbon dated to 1519–1306 calBC (Middle Bronze Age; Table 1; Fig. 7). The infant bones were collected at the front of a rock-debris unit that was cemented by concretions. About one meter away from the burial, a complete baby-bottle was found partially concreted on the room floor (Fig. 9). Furthermore, a complete pyx lid and other well-preserved burial-related jug fragments were found in the

Branch RA between the block slide and the southwestern wall of the cave (Fig. 8b, e).

In rooms 1 and 2, just above the CA and EBA deposits, some layers yielded potsherds dated to the MBA 1–2 based on typochronologically parallels, but without human remains in primary deposition. Radiocarbon dates ranging from 1611 to 1231 calBC were obtained from fauna remains collected from these layers (Fig. 7 and Table 1). No typical settlement features (e.g., post holes, small ditches) were detected in these deposits. On top of the CA and of the partially concreted MBA layers, loose and reworked layers rich in MBA potsherds and dog bones were found. Two bones of dogs found within these layers, SU 18 in Room 2 and SU 9 in Room 1, were radiocarbon dated respectively to the Middle Age and Renaissance (Table 1).

In Room 3, MBA 1 potsherds were found as well (Fig. 6). Some come from layers reworked between medieval times and the present day (Fig. 9, SU 1, 3 and 5). Just below these layers, an MBA layer (SU 6) partly covers the remains of a hearth, containing charcoal, ashes and charred animal bones (SU 7). Inside the ashes, a left radio of a *Sus sp.*, (LS 425) was found and radiocarbon dated to 1493–1231 calBC (Fig. S7a and Table 1).

The hearth was half-covered by a large (40–60 cm) collapsed block that constitutes the base of a concreted fallen-rock assemblage, dividing Room 1 from rooms 3–7 (the “wall” in Fig. 4).



Fig. 8. Excavation and finds. (a) and (c) Human bones from the Copper Age layers, in Room 1. (b) Collecting the potsherds in Branch RA (d). The baby-bottle found in Room RA. (e) The pyx lid and some burial-related potsherds from Branch RA. (Pictures by A. Ferracci and M. F. Rolfo).

5. Discussion

We discuss the results presented above, in the following order: 1) the morphostructural evolution of the La Sassa surroundings; 2) the speleogenesis and neotectonics of the Sassa cave; 3) the seismogenic potential of the studied structures and; 4) the interaction between Protoappenninico and Grotta Nuova facies in the MBA; 5) the utilisation of the cave and 6) the settlement and necropolis patterns.

5.1. Morpho-structural evolution of the La Sassa surroundings

The surroundings of the La Sassa Cave are characterized by a major fault system that was active during the Plio-Quaternary extension. The major faults are NW- and NE-striking and present minor strike undulations resulting in a cumulative minimum displacement of about 0.8–1 km. This is in the order of the major normal faults reported elsewhere in the Volsci Range (e.g., Cardello et al., 2020, 2021 and references therein). Overall, the fault segmentation pattern accounts for E-W and N-S transfer zones (e.g., Morley et al., 1990), which segment the master faults. The fault kinematics recorded both within the Cretaceous carbonate units of the footwall of the major NW-striking fault, and in the Quaternary

breccia in the hanging wall are transtensive. However, they generally accommodate a NE-directed extension. Despite the low deformation rates, i.e., within the Latin Valley (Marra et al., 2021), the focal mechanisms from the earthquakes shaking the region account for the re-activation of the Plio-Pleistocene faults with transtensive kinematics. Besides dip-slip NW-striking faults, of NNE-striking faults with oblique-slip kinematics, our data are consistent with a prevailing NE-oriented sigma-3, as typical of the Apennines (Montone and Mariucci, 2016). As shown elsewhere in the axial zone of the central-southern Apennines, the NW-striking intramontane basins record active NE-directed extension (e.g., Bernard and Zollo, 1989; Montone et al., 1999; Galadini and Galli, 2000; Galadini and Messina, 2004; Chiarabba et al., 2009; Falcucci et al., 2016). However, little is known about active tectonics and the structural control on the distribution of Quaternary sediments and karst development in the internal and coastal part of the Apennines.

As shown in Fig. 10, the fault arrangement controls the location of structural depressions and karstic forms, i.e. the La Sassa graben. In particular, during the Quaternary, NW-striking faults guided the deposition of continental breccia units at the edge of the La Sassa valley. The so formed graben contains Quaternary breccia that, according to our reconstructions based on the present-day tectonic

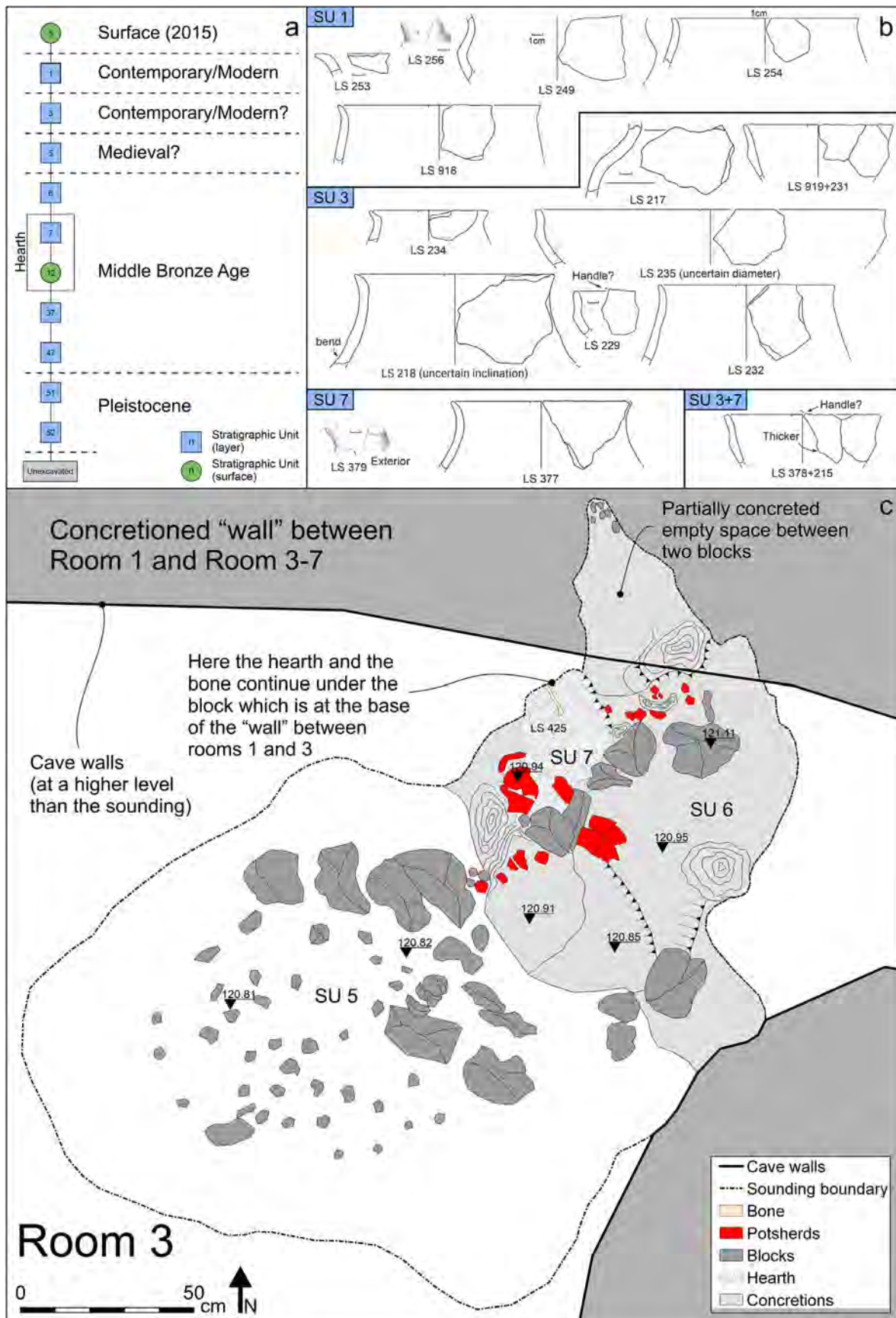


Fig. 9. Archaeological finds in Room 3. (a) Matrix of the sounding in Room 3. (b) Diagnostic potsherds collected in Room 3 (drawings by L. Alessandri), for the parallels see [Table S1](#) (c) Map of the sounding in Room 3. SU 5, soil layer with few MBA impasto potsherds, most of them in a sloping NS positions. One potsherd made of depurated clay, possibly roman

and stratigraphic setting, we consider as syn-tectonic (Fig. 10). As demonstrated by Serva and Brunamonte (2007), the infilling lacustrine to marsh-lagoon deposits are thicker where the effects of subsidence were enhanced. Further, this occurs at the foothill of the Volsci Range, where Quaternary normal faults are reported (Milia and Torrente, 2015) and seismicity localizes (see Section 5.3).

Elsewhere in fold-and-thrust belts, it has reported the effect of tectonics on controlling the paleogeographic and sedimentary environment both in marine (e.g., Cardello and Mancktelow, 2014) and continental hypogeous conditions, which guided the speleogenesis (Ekmekçi, 2005, 2003; Miller, 1996). In particular, Miller (1996) relates the extent and position of karst systems in Belize to a control by major bounding faults with a situation that shares some similarity with the La Sassa Valley. Generally, the architecture of fault zones typically exerts control on fluid flow in the upper crust (Bense et al., 2013; Caine et al., 1996; Rawling et al., 2001; Doglioni et al., 2015) also, from examples exhumed from the seismogenic depth that can affect both thrust (e.g., Perfettini et al., 2010; Dal Zilio et al., 2018; Cardello et al., 2019; Menant et al., 2019) and normal faults (e.g., Clemenzi et al., 2015). The relationships between karst processes and tectonics have been well-explored in the review work of Shanov and Kostov (2015). The role of tectonic elements as fractures and faults on guiding the underground karst systems has been recognized (Goldscheider, 2005; Klimchouk et al., 2012; Klimchouk and Ford, 2000; Pepe and Parise, 2014; Stafford et al., 2005; Šuštersiĉ, 2006).

Similar to our context, in the Ligurian Alps (Antonellini et al., 2019) and a number of other localities, regional tectonic uplift and neotectonics triggered karst development (e.g., Ekmekçi, 2003). For example, small-scale poljes develop along the depression related to the axis of a syncline fold in the Northern Alps (Goepfert et al., 2011). In tectonically-controlled karst contexts with localized fractured zones, the cave shape and the distribution of underground and landscape forms are guided by major faults (Pepe and Parise, 2014; Tîrlă and Vijulie, 2013) (c.f. section 5.6). The control of tectonics on karst development occurs both in epigene (Silva et al., 2017) and hypogene conditions (Cazarin et al., 2019; Ennes-Silva et al., 2016; Klimchouk et al., 2016). The relations among fractures, bedding and faults were established also in a gypsum cave in the Northern Apennines, where they guided the karst epigenesis of a cave (Pisani et al., 2019). However, the constraints provided by the archaeological and paleontological findings and datings are rarely reported in the literature concerning underground neotectonics. In our interpretation, during and after the Quaternary Breccia deposition, the Sonnino surroundings were affected by karstic (e.g., possibly periglacial thermokarst), fluvial and tectonic processes. In this study, we could not constrain the age of the host-rock breccia nor detail the steps of evolution before the CA, however U/Th or C-14 dating on speleothems could better assess the progression of Quaternary tectonics in the area. Yet, we remark that the La Sassa cave could have undergone multiple phases of formation related to the regionally recorded climatic variations (Bini et al., 2020; Boschini et al., 2021), that must be older than our oldest dated bone (i.e., pre- 32,930 calBC) in the upper Pleistocene deposits found within the cave (Fig. 7).

5.2. Speleogenesis stages and neotectonics of La Sassa cave

In light of the 3D speleological and structural surveys of the La Sassa cave, we propose an interpretation that explains the

speleogenesis of the cave. As shown in Fig. 11, the drop-in height level between the averaged roof height of Room 1 and the roof of rooms 3–7, corresponds with the occurrence of morphostructural aligned steps dipping towards the SW and thus of NW- and E-striking thoroughgoing faults that offset the morphology of the cave and its outside (Figs. 3 and 4). As documented, the NW-striking normal faults in the breccia associated with metric-scaled offset, crop out associated with major NW-striking regional faults recording larger offsets (Figs. 4 and 11). In the surroundings of the cave, dm-to metric amount of topographic offset can also be recognized in the topographic articulations of the Quaternary terrace. Those forms can be compared with the structures observed within the cave. In particular, the morphologic offset (4.75 m) is likely to be due to a fault offset related to the E-striking and NW-striking high-angle fault zones with similar orientations as documented on the surface in the surroundings of the cave affecting both the Quaternary rocks and the Cretaceous carbonate groups (Fig. 3, S1). In this perspective, as reported, most of the morphostructural lineaments in the cave can be considered near-surface fault branches of the major normal to oblique normal faults bounding the La Sassa graben. Thus, in our interpretation, we consider the present-day step-wise shape of the cave as resulting from fractured zones and faults prone to roof collapses and concretioning.

Radiocarbon dates on human and fauna remains, together with relative ages based on potsherd typo-chronology, have been used to constrain the ages of the infilling deposits. By correlating this information with the structural data we could indirectly reconstruct the timing of faulting. In the cave, the evolutionary steps retrieved from the interpretation of the events were obtained by analysing the cross-section AB in Fig. 3b,d, which was extracted from the 3D model (Figs. 4 and 11). This has provided the basis for a sketched reconstruction, which aims at establishing the evolution steps related to the development of the cave during the Late Pleistocene, the Copper Age, the Middle Bronze Age and present day.

The resulting structure has been manually restored in Fig. 11 by applying a kinematic inversion of movement along faults, according to their amount of displacement. This is done because a 2D restoration is schematic and implicitly assumes that there is no movement of material into or out of the plane of the section. Besides the structural aspects, our multidisciplinary approach, including the taphonomic and spatial distribution of the entire assemblage, allows to reconstruct the animal and human occupation stages of the cave (Fig. 11; cf. Section 5.5). The upper Pleistocene as well as the CA and MBA sediments are preserved within depositional pockets bounded by fallen blocks constituting rocky concreted walls or concreted fault zones. At the same time, the roof of the cave, far from these edges, is flat and relatively free of concretions. The ages of the infilling deposits are constrained by the sixteen absolute ages and other relative ages presented in this work between the Late Pleistocene and the Renaissance (Table 1), therewith dating the timing of faulting.

During the Late Pleistocene, in a time period corresponding to 32,930 and 30,674 calBC, Rooms 1 and 2 together constituted an ample cave hyena den that allowed a free circulation of the fauna in the cave prior to the onset of concretioning. The lenticular shape of the cave possibly followed a more erodible layer within the Quaternary breccia which dips towards the SW around 20°. As we will discuss later, concretioning is triggered and enhanced by the onset of faulting, which, based on taphonomic data, shortly postdated the

or medieval, has been collected from this layer. SU 6 is a calcite floor with several MBA potsherds. The latter were embedded in the concretions and slightly sloping from north to south. SU 7 consists of ashes, charcoal and charred animal bones. The deposit fills an artificial cavity (cut) in the calcite floor. At the bottom of this cavity, just below the ashes, a layer of potsherds was intentionally placed in flat position. (Drawing by E. Fazi, A. Ferracci and R. Malinconico).

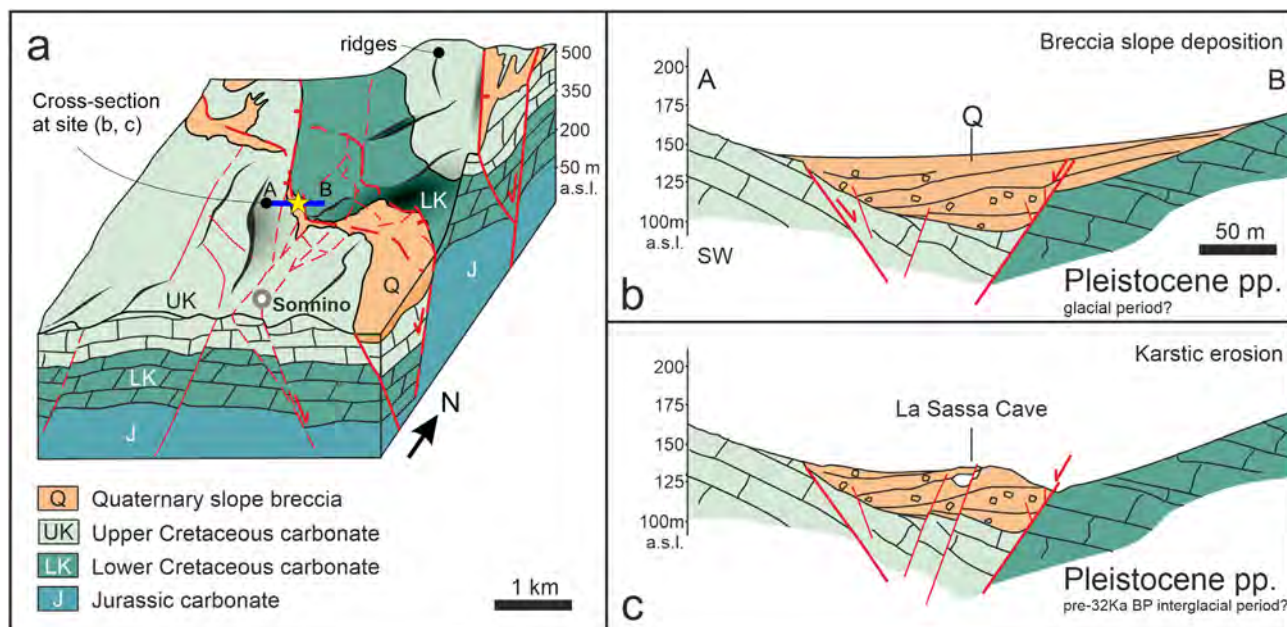


Fig. 10. Reconstruction of the La Sassa Valley. A) Sketch of the 3D setting of the La Sassa Valley and surrounding areas characterized by an articulated horst and graben structure. b-c) 2D schematic restoration of the cross-section presented in Fig. 3d B) The infill breccia layers of the La Sassa graben is likely coeval with the erosion of the mountain ridges made of Cretaceous carbonates during the syn-tectonic evolution of the graben. c) pre-32.9 ka karstic erosion affected the breccia generating the La Sassa cave.

death of the bears in Room 6. Further, as the bear(s) were found in a space that is much smaller (20–30 cm in height; Fig. 6) than the size of a living-brown bear (70–150 cm), this implies that the accommodation space for a winter shelter was compartmentalized and reduced by concretioning after their death. From a structural and speleological point of view we conclude that the concretion process started after the death of the bear and during the use of the cave as a hyena den. The radiocarbon dates suggest that concretioning started after 32,930 calBC. Considering that the bear bones found in Room 6 are free of cutmarks and gnawings, they have naturally died in this inner area of the cave, where they probably retreated to hibernate (Fiorillo, 2016). Thus, although the radiocarbon date of hyenas and bears overlap in geologic time, it is unlikely that they actually made use of the cave at the same time. In our interpretation, we suppose that the rejuvenated shape of the cave triggered the partial remobilization of the upper Pleistocene deposits, that were not yet concretioned. In particular, in Room 3, the chaotic distribution and the vertical position of the hyena bones point at a reworked deposit, that possibly did slide from the upper Room 1. However, close to the faults, concretioning of the Pleistocene hyena-bearing deposits shows that this process started already during their presence, suggesting that faulting and remobilization could have onset in the cave during this stage.

During the Copper Age (CA), in a time period comprised between 3300 and about 2000 calBC, the cave had already experienced much of the offset of the normal faults as it was already compartmentalized in progressively smaller rooms towards the SW with the footwall of faults possibly exposing the upper Pleistocene rocks. Meantime those fault walls could have already been concretioned. In the CA, as constrained by the archaeological finds and four radiocarbon ages, the cave was used as a burial place (see section 5.4).

In the Middle Bronze Age (MBA), between 1900 and 1200 BCE, the cave was experiencing widespread concretioning on both the floor and along the major fault-steps (i.e., Room 3 and 1). In other areas of the La Sassa Cave, where the rock debris was not completely “frozen” by the concretions, the rocks filled the lower

portion of the cave, possibly reworking finds of CA and EBA. Remobilization of the fallen blocks occurred before concretioning set on, as suggested by the disposition of the MBA baby burial in Room RA. The four radiocarbon age constraints from this period derive from the finds of a hearth leftover and possibly cultic activities whose implications are discussed in Section 5.5.

In more recent times, comprised between the Bronze Age (1233 calBC) and the Middle Age (1222 calAD), we highlight the presence of a fracture crosscutting a column belonging to the post-MBA concretioned “wall” between Room 1 and Room 3–7. This fracture, also schematically reported in Fig. 11 is partially healed by the growth of new speleothems representing a relatively recent effect of faulting, which could either be due to local activity or represent a coseismic effect of nearby earthquakes. The rock fall and concretioning at fault zones progressively generated a series of walls that hampered the rock debris to slide further downward and completely fill the space, acting as a dam (e.g., covering the MBA hearth in Room 3). Accordingly, we interpret the fault healing documented in rooms 1–3 on the post-MBA dividing wall as the most recent faulting effect in the cave. Further, the collapses near the fault zones had occurred before the emplacement of the concretioned “wall” between Room 1 and Room 3–7, which formed slightly after the MBA 1–2. In particular, we recognize that the fault intersection occurring at the cave entrances and the coexistence of increasing fracturing with concretioning at the southwestern edges of the rooms of the cave, intimately tighten the relationship between tectonic processes (faulting and fracturing) and the internal karst development. This “dam” has prevented the medieval unconsolidated debris to fall in the lower rooms. This suggests that the latest concretioning, to which we can possibly date the most recent healing event on the faulted column, could have occurred in a time comprised between the Middle Bronze Age and the Middle Age (cf. Table 1 and Fig. 4).

5.3. Seismogenic potential

The La Sassa morphostructural evolution during the Late

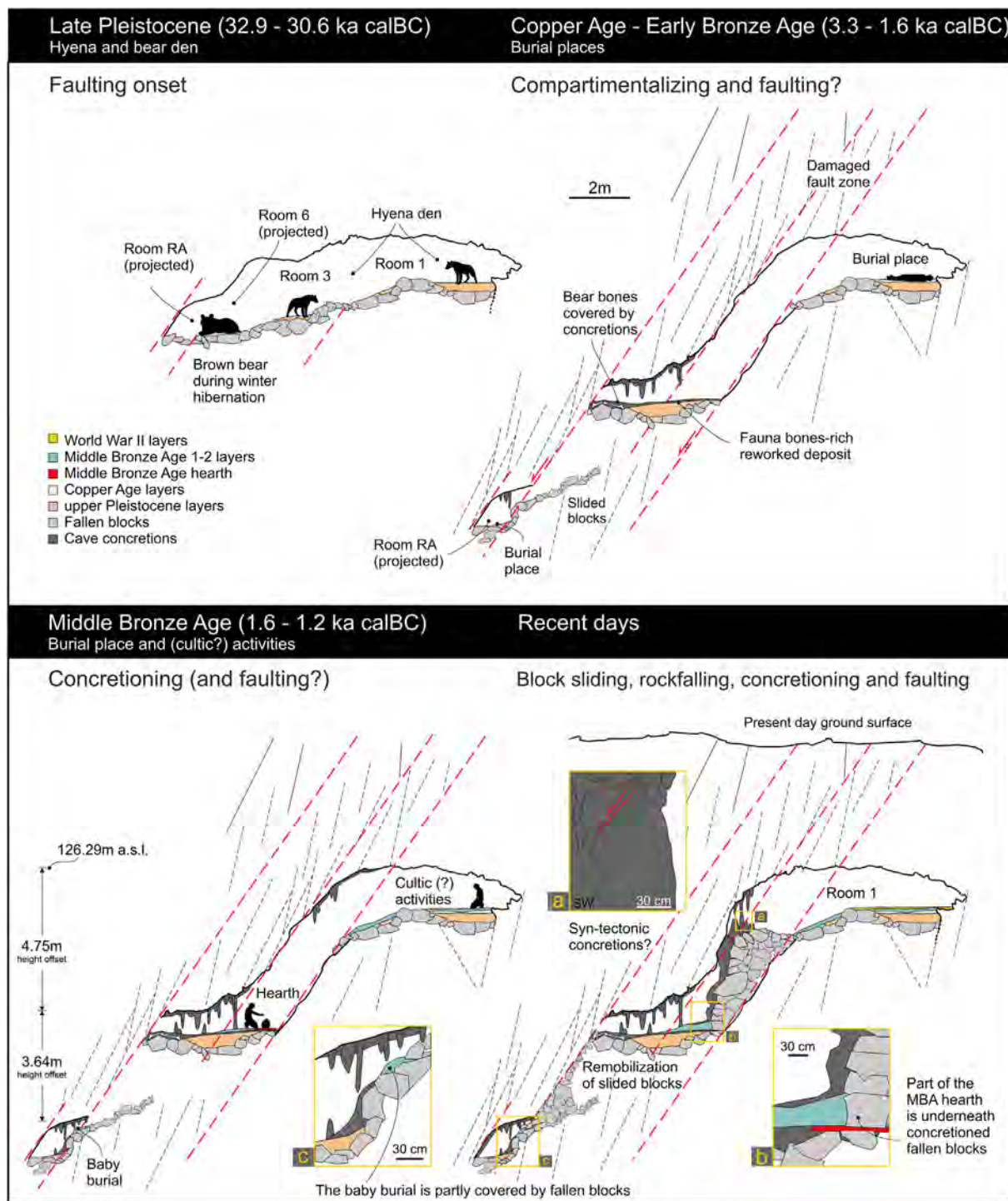


Fig. 11. Evolution of La Sassa cave. Reconstruction of the morphologic and structural evolution of the La Sassa cave from the Late Pleistocene up to the present day. The cross-section of the cave (C in Fig. 4) has been extracted from the photogrammetric 3D model, that identifies a step-wise shape of the cave due to normal fault steps, with the projected add of Room RA. The room for bears and hyena is reconstructed as virtually free of large concretions with a less prominent shape of the cave. In its Copper Age-Early Bronze Age, Middle Bronze Age and present-day shape, the cave has become affected by faulting and progressively infilled by collapsed blocks, concretions. Layer trends are schematic but describe the different steps of the syn-sedimentary evolution related to normal faulting in the cave. Details in the yellow bounded insets are referred to important finds (i.e., CA baby burial on MBA remobilized and concretioned debris; column cross-cut by a fault and later partially healed; MBA hearth underneath a fault-related concretioned-wall). (For interpretation of the references to colour in this figure legend, the reader is referred to the Web version of this article.)

Pleistocene to more recent times can possibly be used to provide constraints to the paleogeographic evolution of the Pontina Plain (van Gorp et al., 2020) and nearby areas (cf. section 5.6). In particular, by contextualizing and scaling our faults into a present-

day dynamic context, we can attempt to estimate the seismogenic potential of the La Sassa faults.

In the vicinity of our study area, within the Pontina Plain (about 15–25 km to the west, Fig. 1), the distribution of the instrumentally

recorded earthquakes clearly shows (W)NW- and NNE-striking 7–10 km elongated clusters with major events up to Mw 3.8 (cf. <http://terremoti.ingv.it/search>). As also reported by Marra et al. (2021), despite the localization error of the seismic source, the two strongest earthquakes seem to have occurred at the intersection between the two above mentioned seismic alignments. Similar to what hereby described on the transfer faults of La Sassa (see section 4.1), the main earthquakes in the Pontina Plain also show a significant strike-slip component. Further, concerning their depth, most hypocentres occur in the first 10 km and, as typical of karst settings, a complex pattern of water flow occurs (Boni et al., 1981). This information contributes scaling the active faults near Sonnino (Figs. 1 and 2), which can be compared with the Quaternary faults cropping out in the Volsci Range (Fig. 1). The latter accumulated an estimated offset in the order of 1 km and along strike fault length in the order of 10–12 km occur (Cardello et al., 2020), which is geometrically and compositionally similar to what studied in the exhumed examples of seismogenic faults in carbonates elsewhere in the Apennines and in the Helvetic Alps (Cardello and Tesei, 2013; Cardello and Mancktelow, 2015; Clemenzi et al., 2015), where as demonstrated by groundwater studies deep fluids are involved (Barberio et al., 2021). As shown at La Sassa, considering that Quaternary faults are subdivided into segments that rarely exceed the length of about 3–4 km, we attribute for the Wells and Coppersmith (1994) empirical correlation line a possible maximum expected earthquake of about 5.1 Moment Magnitude (Mw). However, considering the total fault displacement along the whole length of the major normal fault, if the fault offset is explained as a cumulative coseismic slip, then earthquakes with a magnitude up to 5.8 Mw could be expected. This estimate is comparable with the magnitude of the most relevant regional earthquakes of Anzio and Ceccano that reached respectively a reconstructed magnitude of Mw 5.2 and 5.6 (Fig. 1) (Rovida et al., 2020). Also, these findings support the model of a multi-phased tectonic uplift affecting the coast of Latium (Karner et al., 2001; Marra et al., 2016, 2019a) with differential uplift between the Anzio-Circeo coastal ridge and the subsiding inner sector of the Pontina Plain (Marra et al., 2019b, 2020; Sevink et al., 2020) during the last 250 ka. Recent findings in low-seismicity sectors of the western Mediterranean Sea show that Late Pleistocene to Holocene tectonics are supported by significant regional uplift (e.g., Sardinia; Casini et al., 2020), which has been recently detected in zones/areas near our study area (cf., Section 2; Delchiaro et al., 2020) and attributed to slab break-off (San Jose et al., 2020).

5.4. Interaction between Protoappenninico and Grotta Nuova facies in the MBA 1

The potsherds recovered in the sounding of Room 3 can be all dated to the subphase MBA 1 (Table S1), with only one exception (LS 234). They all have close parallels with the Protoappenninico facies, thus confirming the presence of this facies in our study area (Damiani, 1995). The ceramic record was similar in sounding SP, in Room 1 (Fig. 4), but here some potsherds could be dated more precisely either to a very early moment of the Protoappenninico facies, likely in the MBA1A, or to the MBA1B (Alessandri et al., 2018). While the more ancient potsherds can be exclusively attributed to the Protoappenninico facies (from the South), a few MBA1B potsherds show parallels with the Grotta Nuova facies (from the North). Synthesising, the potsherds from both soundings point to an exclusive Protoappenninico ceramic culture at the beginning of the MBA, while in the MBA1B traces of contacts with the northern facies are evident. In the near-by Vittorio Vecchi cave (Fig. 1 and) the situation is reversed. Here, according to the authors, the MBA1A potsherds exclusively belong to the Grotta Nuova facies and the

MBA1B potsherds show the first traces of contact with the Protoappenninico facies (Guidi, Rosini, 2019). The ceramic record therefore suggests that in the MBA1A the Amaseno valley, which runs between the Lepini and Ausoni Mounts (Figs. 1 and 2) constituted the boundary between the two facies. This would imply that in the MBA1B the populations south and north of the valley maintained cultural contacts. To test the hypothesis of exchange of goods and/or people isotopic (Sr) analyses on the human remains of La Sassa are underway. Unfortunately, potsherds from Colle Colanero, Mola dell'Abbadia and Valle Fredda (Fig. 2) remain unpublished, so their stylistic traits cannot be checked (Anastasia, 2007). Although potsherds from Colle Pistasale (Cancellieri, 1986) show some Protoappenninico influence, at least during MBA 1, they are too few to infer a chronological development. The overall picture fits with the progressive increase in the mixture of stylistic traits, already observed during the MBA in all of central-south Italy: in the subsequent MBA 3 (around 1400–1300 BCE) the entire area will be characterised by the same Appenninico facies (Macchiarola, 1995; Pacciarelli, 2001).

5.5. The utilisation of the cave

The evidence about the use of the La Sassa cave during the Bronze Age is discussed below, in order to both contextualize our archaeological finds and to constrain the tectonic of the cave. The utilisation of caves in Bronze Age central Italy has been long debated (Cazzella and Guidi, 2016; Cocchi Genick, 1998, 2002; Guidi, 1992; Guidi and Rosini, 2019; Ricciardi, 2012). Hypotheses range from water cults to practical uses related to burials, temporary shelters, or economy (e.g., sheepfolds), to name a few. In our case, the CA and EBA evidence from La Sassa points to a funerary use of the cave. It must be noted that in central Europe, the presence of Bronze Age items in caves, including human remains, has often been interpreted as the results of ritual offering. The missing anatomical connections, which is also quite common in Italy (including La Sassa), was one of the main points which led the authors to interpret them as the results of human sacrifice, sometimes associated with cannibalism (Orschiedt, 2012). However, during the excavation of the Vittorio Vecchi Cave (Fig. 2c and d) (Guidi and Rosini, 2019), the authors noticed that the potsherds and the bones were better preserved along the wall of the cave, compared to those found in the centre of the main room. This evidence led the author to hypothesise that the corpses were first put along the walls of the cave and later transferred to the centre of the room to make space for new burials. This process would explain the loss of anatomical integrity of most of the human skeletons. The evidence from La Sassa points to the same process. The presence in the skeletal record of all the anatomical districts, including the smaller bones, indicates a primary deposition in the cave, subsequently manipulated in the same place or in the immediate proximity. Besides, as for sex and age, the record in La Sassa is the expected outcome of several extended family in a contemporary village. Finally, in La Sassa no traces of cannibalism or ritual sacrifices, like cut-marks and perimortal breakage patterns have been detected on human bones.

In MBA 1–2, the layers in rooms 1 and 2 show very few human remains, that moreover originate from the lower CA and EBA layers. Thus, a funerary context can be easily ruled out. Moreover, as shown by the geological reconstruction, the hearth discovered in the Room 3 was likely at the same level or just a little beneath the MBA 1–2 deposits and certainly was in use when rooms 1, 2 and 3 formed a unique space (Fig. 11). In central Italy, hearths are a common discovery in MBA cave contexts. Since the current Italian interpretative framework almost excludes a residential use of the caves in the Bronze Age (Cazzella and Guidi, 2016), these features

are usually considered traces of ritual activities. Nearby, they have been found in the Vittorio Vecchi (Sezze, Guidi and Rosini, 2019), Regina Margherita (Figs. 1 and 2) (Colleparado, Angle et al., 2010) and Pastena (Figs. 1 and 3) (Pastena, Angle et al., 2014) caves. In the Vittorio Vecchi cave, the presence of hearths and charred seeds in the main room, close to the human remains, led the author to hypothesise the presence of ritual activities (Guidi and Rosini, 2019). In the case of Regina Margherita and Pastena, the zooarchaeological record has been carefully studied and proved to be a fundamental proxy to interpret the archaeological deposits (Silvestri et al., 2018). In the Pastena cave, the fire and cut marks and the kill-off patterns of the domesticated fauna bones indicate recurring meat consumption. According to the authors, this evidence, together with the depositional context, a small and quite inaccessible and dark room, points to a ritual activity. In the Regina Margherita cave, the hearths were found near the entrance and associated with domesticated animal bones. The area was slightly separated from the burial area, which is located in the inner portion of the cave, thus the authors hypothesise that offerings took place related to the mortuary contexts.

In the rest of Europe, like in Italy, hearths were found to be often associated with burial areas and often interpreted as traces of ritual activity (Harding, 2000) like in the cases of the Duffaits cave, in France (Gomez de Soto, 1973) and the Bezdanjača cave in Croatia (Drechsler-Bizic, 1980). On the other hand, especially in France, Bronze Age caves are mainly considered dwellings or dwelling annexes (Orschiedt, 2012; Treffort, 2005), thus hearths in caves have also been considered as related to domestic activities. It has already been noted that these opposite interpretations, rather than originating from different archaeological records, seem to be the effect of diverse scholarly traditions (Silvestri, 2017). However, as Brück (1999) pointed out, the dichotomy between ritual and domestic activities might well be a Western perception grounded in the post-Enlightenment rationalism which opposes the functional (secular) to the non-functional and irrational (ritual). The issue is also interwoven with the definition of the word “ritual” about which there is no general consensus among anthropologists. The definition of rituality ranges from the expression of fundamental propositions linked with religious beliefs (focusing on the message) (Rappaport, 1999) to performances according to precise conventions (focusing on the procedure) (Turner, 1969).

In 2005, Bradley tried to overcome the methodological deadlock. Following Brück's arguments, he suggested that rituality might be considered a performance defined by its own conventions where certain parts of life are selected and given particular emphasis (Bradley, 2005). In such a way, the distinction between domestic and ritual activity would eventually disappear and archaeologists can monitor the development of ritualization as part of social and political trajectories.

From this perspective, the MBA layers and the hearth in rooms 1–3, can be considered the outcome of a ritual that involved food consumption just above or close to the human bone deposit. The human bones were likely visible, since there was no additional soil between the CA/EBA and the MBA deposit. The ongoing study on the associated fauna remains (more than 5000 bones) and on the complete potsherd assemblages would certainly shed new light on this issue, helping to unveil the social framework.

At the end of this phase (MBA 2), the burial area shifted to the inner portion of the cave (Room RA) and perhaps in other non-yet investigated areas, like the north-west portion of Room 1, still occupied by a more recent block-debris. In Room RA, a single MBA (infant) burial has been recovered. In particular, these remains were found dispersed in a very small area, with no traces of other individuals. This latter evidence points to a single deposition in Room RA that later, during the remobilization of the underlying sliding

blocks, was partly disturbed.

5.6. Settlement and necropolis patterns

So far, no CA or EBA settlements have been reported in the La Sassa valley. The nearest MBA known settlement is Mola dell'Abbadia, which is at around 46 min walking-time (Fig. 12). Colle Colanero and Colle Pistasale are at 50–60 min (Fig. 12a).

The reciprocal distance between the settlements is quite regular, with an average of about 50 min walking-time, thus enclosing territories with a radius of about 25 min. In southern Lazio, in MBA 1, territories with a similar radius (around 26 min) have also been identified near Anzio (Fig. 1) (Alessandri, 2013). The 2–3 km radius territories, which equals 24–36 min in level terrain, is recognized as a recurrent worldwide catchment radius, in a package that also includes a maximum of 5 km and a minimum of 1–2 km. Already in 1976, in his study about the early Mesoamerican villages, Flannery provided an elegant explanation for these values, arguing that they were the results of successive divisions (tessellation) of the available area (Flannery, 1976). Colonising a new area, farmers tend to develop their activities in a radius of around 5 km (60 min walking-time). Thus, a progressive infill of the available area tends to produce a network of settlements about 10 km apart. In a context of demographic growth, when all the available soil was already occupied, new settlements must carve out their territories at the expense of the older villages. A 5 km radius fragmented by 2 gives a 2–3 km territory radius and, if the process goes on, a subsequent 1–2 km radius. As Flannery pointed out, the settlements with a 5 km radius had likely more land and, consequentially, resources than needed. The 1 km radius could instead be interpreted as a symptom of unusual pressure on the land. In this regard, the 2–3 km radius seems to be balanced and sustainable. Not surprisingly, this value can be found in Europe, in different periods. Territories with a 2 km radius (which equals 24 min in level terrain) were proposed by Ellison and Harris (1974) for southern England between the Bronze Age and the early medieval period. A radius between 1 and 2 km (12–24 min in level terrain) also characterised the Early Neolithic villages in Thessaly (Perlès, 1999). Slightly wider territories (2.5 km, around 30 min walk) have been reconstructed for the Bulgarian Neolithic tells (Dennel, Webley, 1975), and the Classical period in Boeotia and Attica (Bintliff, 1999, 2009). Later, the same radius was proposed for medieval settlements in the Netherlands, France and Britain (Davies, 1988; Heidinga, 1987; Pounds, 1974). In 1999, Bintliff began to apply the conceptual tools of the Complexity Theory (Bintliff, 1999) to the archaeological interpretation. The Complexity Theory aims to explain how complex biological and physical systems tend to converge on stable or semi-stable configurations, named Strange Attractors (Lewin, 1992). In the general process of successive land tessellation described above, he identified three Strange Attractors: the first is the tendency of dry farmers to concentrate their activity in a 5 km, or 1 h walking-time, as already noted by Flannery. The second is the tendency of settlements to split up when they reach about 150 individuals. This seems to be a critical threshold for the so-called face-to-face communities both in social (Forge, 1972) and physical anthropology (Dunbar, 1996). In face-to-face communities the social relations are direct and divisions in subgroups or social classes are not necessary to preserve internal cohesion; when this number is surpassed, the community tends to differentiate internally or to split up (fission). The third Strange Attractor is the tendency to converge to territories with a 2–3 km radius, like in the case of the La Sassa cave, which enclose adequate resources to sustain the settlement needs also in the case of resource restraints. In 2013, Alessandri already suggested that the fission phenomenon could explain the MBA settlement pattern in the study area (Fig. 2;

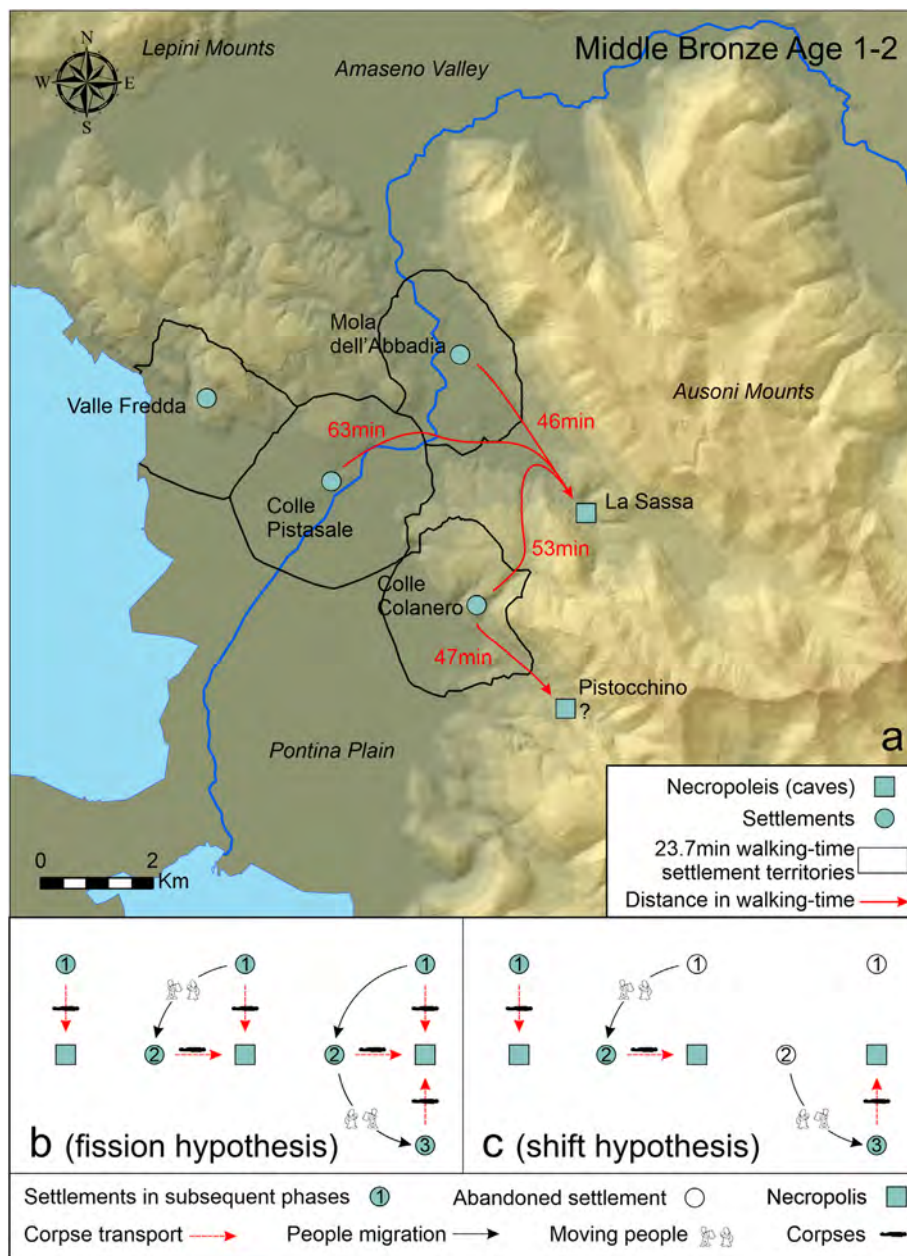


Fig. 12. Settlement patterns in the Middle Bronze Age 1–2 around La Sassa cave. A) Reconstruction of the territories of the settlements near La Sassa cave and their mutual distances. b-c) Two hypotheses about the development of the settlement patterns (moving people symbol from Cavazzuti et al., 2019).

Fig. 12b). However, he also suggested an alternative hypothesis: these villages could have periodically shifted in search of “fresh” terrains, that were not impoverished by agricultural use (Fig. 12c). In this perspective, Colle Colanero, Colle Pistasale and Mola dell’Abbadia (Fig. 12a) might have been the archaeological footprints of the same community moving to unexploited lands, caught at different times although all included in the MBA 1–2 (Alessandri, 2013). To this model, we can now propose the existence of a fourth Strange Attractor. The radiocarbon dates suggest that, even in a settlement pattern scheme where one or more villages periodically move around, the necropolis of La Sassa continued to be used for at least 1400 years, both as a burial place or as a site where to perform possible ritual activities. This should not be surprising since the presence of caves with an easy entrance and a considerable amount of space available such as La Sassa is rare and at the

moment the CA to MBA funerary practices seem to be restricted only to natural or artificial (smaller) caves. Further, the distance between the settlements and the cave remained quite stable, with an average of 54 min. MBA potsherds, in reworked Roman layers with Republican ex-voto objects, have also been found in the Pistocchino cave (Alessandri and Rolfo, 2015), which is about 47 min from the settlement of Colle Colanero. The cave has not been further investigated, but it is likely that it previously served as a ritual or burial place, like the majority of central Italian caves. A partly similar situation, based on Sr and O isotope analyses, has been proposed for the EBA necropolis of Sant’Eurosia (Cavazzuti et al., 2019) in the Po Plain, where the dispersed isotope ratios indicate that the buried people were rather mobile and their provenance had to be placed in a hinterland of about 20–50 km radius, which in a flat terrain equals 4–10 h of walking-time. In this

case, the necropolis was used for a much shorter time, but it still worked as a “persistent place” in the settlement pattern.

6. Conclusions

We hereby synthesize the outcomes of a novel investigation method comprehensive of geomatic, structural geology, palaeontological, archaeological and radiometric data applied to solve the morphostructural evolution of a cave in an area with unconstrained Quaternary evidence. This method enabled us to recognize:

- a step-like shape of the cave that is associated with normal faults with similar orientation also occurring in the surroundings;
- Late Pleistocene (32,930–30,6744 calBC) hyena and bear bones, which were partially to fully embedded in concretions near the wall of a major fault marking the onset of syn-sedimentary faulting in the cave;
- syn-sedimentary pockets generated within small step-like metric-scaled basins preserving rich archaeological finds belonging to the Copper Age (CA, 3300–2000 calBC) and the Early and Middle Bronze Age (EBA–MBA, 1900–1200 calBC);
- Middle Bronze Age to Medieval collapse of blocks and concretions occurring at approaching fault zones.

In our interpretation, the CA deposits progressively infill rooms, while the concretioned collapse covering the MBA hearth is evidence of crack-and-seal processes along a secondary fault zone of a segmented major normal fault of the Volsci Range with cumulative subsurface rupture length reaching up to 10–12 km and displacement in the order of 0.8–1 km, which could possibly be capable of generating an earthquake of magnitude M_w comprised between 5.1 and 5.8 depending on the fault segmentation. The structural evidence is relevant for understanding the speleogenesis from the Late Pleistocene and the human occupation of the cave.

The archaeological evidence suggests that in the area:

- the boundary between the Protoappenninico and Grotta Nuova facies might be placed along the Amaseno valley;
- The long-lasting process of stylistic melting between Protoappenninico and Grotta Nuova facies starts in the MBA1B;
- The cave was used as a burial place from CA to MBA 1–2 and possibly to perform ritual activities in the MBA 1–2;
- In the MBA, the cave acted as a “persistent place” within a developing settlement pattern.

Overall, these results set the timing of faulting and thus represent the first neotectonic evolution ever documented in the internal Central Apennines nearby Rome. The outcome is of regional relevance as Late Pleistocene to Holocene/Anthropocene neotectonics were poorly constrained by the structural studies of the Tyrrhenian coast of Latium, due to the rarity of outcrops of syn-tectonic rocks and possibly to a less active seismic context. As a result, the La Sassa findings provide temporal constraints to the recent regional tectonic evolution. This study sets the ground for further seismic hazard assessment in a region inhabited by about 0.4 million people.

The specific attention for post-depositional processes improved our understanding of the interplay between geological processes and human use of the cave and allow us to put forward some hypotheses on the local to regional development of the human landscape. We believe that the methodology adopted in this study has the potential to unveil (pre)historical processes and to constrain neotectonic evolution also in similar contexts worldwide.

Declaration of competing interest

The authors declare no competing interests.

Acknowledgements

We would like to thank the Soprintendenza Archeologia, Belle Arti e Paesaggio per le Province di Frosinone, Latina e Rieti, the municipality of Sonnino and the speleological groups Gruppo Grotte Castelli Romani, Shaka Zulu Subiaco and Speleo Club Roma. We thank Fabrizio Marra, and Silvano Agostini for the critical reading of the manuscript. We are also deeply grateful to Katia Francesca Achino, Micaela Angle, Gianni Carroccia, Nicoletta Casieri, Gianni Celani, Andrea Cesaretti, Paolo Dalmiglio, Flavio De Angelis, Luciano De Angelis, Francesco Di Mario, Angelica Ferracci, Alessandro Guidi, Elia Mariani, Fabrizio Marra, Gianluca Mellandri, Jessica Merenda, Angelo Procaccianti, Marco Romboni, Leonardo Salari, Damiano Santinelli, Letizia Silvestri and Roberta Tozzi.

Funding

This work was supported by Nederlandse Organisatie voor Wetenschappelijk Onderzoek (NWO Free Competition grant 360-61-060).

Author contributions

L.A. and G.L.C. were involved equally in designing the study, acquiring and analysing the data, writing the manuscript and preparing figures. L.A. and M.G. contributed to fund acquisition. V.B., S.D.P., F.D.C., F.M., M.O., S.T., designed, executed and processed the network necessary for the geodetic framing of the 3d model. They have also carried out the surveys and calculations necessary for the realisation of the model. A.F., M.G., M.F.R. studied the palaeontological remains. P. A.J.A. and G.S. reviewed all the manuscript. All authors contributed substantially to drafts and gave approval for publication.

Data and materials availability

All data needed to evaluate the conclusions in the paper are present in the paper and the Supplementary Materials. The finds from La Sassa cave are stored in the Archaeology Laboratory of the University of Tor Vergata, Department of History, Culture and Society (Rome, Italy).

Appendix A. Supplementary data

Supplementary data to this article can be found online at <https://doi.org/10.1016/j.quascirev.2021.107067>.

References

- Accordi, B., Segre, A.O., Cocozza, T., Angelucci, A., Sirna, G., Farinacci, A., 1966. Sheet 159 Frosinone of the Geological Map of Italy at L:100'000, second ed. Servizio Geologico d' Italia, Roma.
- Agostini, S., Forti, P., 1982. Indagine sismotettonica dell'area carsica a Sud Est di Latina (M. Ausoni e M. Ernici) con metodi speleologici - contributi alla realizzazione della Carta Neotettonica d'Italia. Progetto Finalizzato Geodinamica pubb 513 (CNR).
- Alessandri, L., 2013. Latium Vetus in the Bronze Age and Early Iron Age// *Latium Vetus nell'età del Bronzo e nella prima età del Ferro*. BAR Int. Ser. 2565 (Oxford).
- Alessandri, L., 2019. The early and Middle Bronze Age (1/2) in South and central Tyrrhenian Italy and their connections with the Avellino eruption: an overview. *Quat. Int.* 499, 161–185. <https://doi.org/10.1016/j.quaint.2018.08.002>.
- Alessandri, L., Rolfo, M.F., 2015. L'utilizzo delle cavità naturali nella media età del Bronzo: nuovi dati dal Lazio meridionale. *Boll. Unione Stor. e Arte* 10, 109–126.
- Alessandri, L., Achino, K.F., Gatta, M., Rolfo, M.F., Silvestri, L., 2018. Grotta La Sassa

- (Sonnino). Poster presented at: siti chiave tra antico e inizi medio Bronzo nel Lazio e in Campania. Nuovi dati e nuove date, 28.6.2018, Naples (Italy).
- Alessandri, L., Achino, K.F., Attema, P.A.J., de Novaes Nascimento, M., Gatta, M., Rolfo, M.F., Sevink, J., Sottili, G., van Gorp, W., 2019. Salt or fish (or salted fish)? The Bronze Age specialised sites along the Tyrrhenian coast of Central Italy: new insights from Caprolace settlement. *PLoS One* 14.
- Alessandri, L., Baiocchi, V., Del Pizzo, S., Di Ciaccio, F., Onori, M., Rolfo, M.F., Troisi, S., 2020. A flexible and swift approach for 3D image-based survey in a cave. *Appl. Geomatics*. <https://doi.org/10.1007/s12518-020-00309-4>.
- Allen, J.R.M., Watts, W.A., Huntley, B., 2000. Weichselian palynostratigraphy, palaeovegetation and palaeoenvironment; the record from Lago Grande di Monticchio, southern Italy. *Quat. Int.* 73–74, 91–110. [https://doi.org/10.1016/S1040-6182\(00\)00067-7](https://doi.org/10.1016/S1040-6182(00)00067-7).
- Anastasia, C., 2007. L'evoluzione dell'insediamento nelle valli dell'Amaseno e dell'Ufente nell'età del Bronzo e del Ferro. In: *Atti Della XL Riunione Scientifica Dell'Istituto Italiano Di Preistoria e Protostoria, Strategie Di Insediamento Fra Lazio e Campania in Età Preistorica e Protostorica*, pp. 877–881.
- Angelucci, A., 1966. La serie miocenica della Media Valle Latina. *Geol. Rom.* 5, 425–452.
- Angle, M., Catracchia, F., Cavazzuti, C., Celletti, P., Malorgio, M., Mancini, D., 2010. La grotta Regina Margherita a collepardo (Frosinone). *Lazio e Sabina* 6, 381–393.
- Angle, M., Rolfo, M.F., Fusco, I., Silvestri, L., 2014. New investigations at the cave of Pastena (Frosinone). *Report 2012. Lazio e Sabina* 10, 205–211.
- Antonellini, M., Nannoni, A., Vigna, B., De Waele, J., 2019. Structural control on karst water circulation and speleogenesis in a lithological contact zone: the Bossea cave system (Western Alps, Italy). *Geomorphology* 345, 106832. <https://doi.org/10.1016/j.geomorph.2019.07.019>.
- Attema, P.A.J., Alessandri, L., Bakels, C., Doorenbosch, M., Field, M., Van Gorp, W., De Haas, T., Van Leusen, M., Tol, G.W., Sevink, J., 2019. Vecchie e nuove ricerche multidisciplinari nel territorio di Sezze e nelle zone adiacenti (Agro Pontino, Lazio). *IpoTESI di Preist* 11, 103–118. <https://doi.org/10.6092/issn.1974-7985/9902>.
- Barberio, D., Gori, F., Barbieri, M., Boschetti, T., Caracausi, A., Cardello, G.L., Pettita, M., 2021. Understanding origin and mixing of deep fluids in shallow aquifers and possible implications for crustal deformation studies: san Vittorino Plain. *Central Apennines Appl. Sci.*
- Basili, R., Valensise, G., Vannoli, P., Burrato, P., Fracassi, U., Mariano, S., Tiberti, M.M., Boschi, E., 2008. The Database of Individual Seismogenic Sources (DISS), version 3: summarizing 20 years of research on Italy's earthquake geology. *Tectonophysics* 453, 20–43. <https://doi.org/10.1016/j.tecto.2007.04.014>.
- Bense, V.F., Gleeson, T., Loveless, S.E., Bour, O., Scibek, J., 2013. Fault zone hydrogeology. *Earth Sci. Rev.* 127, 171–192.
- Bernard, P., Zollo, A., 1989. The Irpinia (Italy) 1980 earthquake: detailed analysis of a complex normal faulting. *J. Geophys. Res.: Solid Earth* 94 (B2), 1631–1647.
- Bini, M., Zanchetta, G., Drysdale, R.N., Giaccio, B., Stocchi, P., Vacchi, M., Hellstrom, J.C., Couchoud, I., Monaco, L., Ratti, A., Martini, F., Sarti, L., 2020. An end to the last interglacial highstand before 120 ka: relative sea-level evidence from infreschi cave (southern Italy). *Quat. Sci. Rev.* 250, 106658. <https://doi.org/10.1016/j.quascirev.2020.106658>.
- Bintliff, J.L., 1999. The origins and nature of the Greek city-state and its significance for World settlement history. In: *Actes de La Table Ronde Internationale Organisée Par Le Centre Jean Bérard et L'Ecole Française de Rome Naples*, pp. 27–29. Octobre 1994.
- Bintliff, J.L., 2009. Catchments, settlement chambers and demography: case studies and general theory in the Greek landscape from Prehistory to Early Modern times. In: Favory, F., Nuninger, L. (Eds.), pp. 107–117.
- Blanc, A.C., 1935. Stratigrafia del canale Mussolini nell'Agro Pontino. *Atti della Soc. Toscana di Sci. Nat. Process. Verbali* 44, 52–56.
- Blanc, A.C., 1954. Resti fossili neandertaliani nella Grotta del Fossellone al Monte Circeo: Circeo IV. *Quaternaria* 1, 171–175.
- Blanc, A.C., Segre, A., 1953. Excursion au mont Circé. In: *IV Congrès International, Guide INQUA (International Union for Quaternary)*.
- Boni, C., Bono, P., Calderoni, G., Lombardi, S., Turi, B., 1980. Indagine idrogeologica e geochemica sui rapporti tra ciclo carsico e circuito idrotermale nella Pianura Pontina. *Geol. Appl. Idrogeol.* 15, 204–247.
- Bordoni, P., Valensise, G., 1999. Deformation of the 125 ka marine terrace in Italy: tectonic implications. *Geol. Soc. London, Spec. Publ.* 146, 71–110.
- Boschin, F., Columbu, A., Spagnolo, V., Crezzini, J., Bahain, J.J., Falguères, C., Benazzi, S., Boscato, P., Ronchitelli, A., Moroni, A., Martini, I., 2021. Human occupation continuity in southern Italy towards the end of the Middle Palaeolithic: a palaeoenvironmental perspective from Apulia. *J. Quat. Sci.* <https://doi.org/10.1002/jqs.3319>.
- Bradley, R., 2005. *Ritual and Domestic Life in Prehistoric Europe*. Routledge, London.
- Brock, F., Higham, T., Ditchfield, P., Ramsey, C.B., 2010. Current pretreatment methods for AMS radiocarbon dating at the oxford radiocarbon accelerator unit (orau). *Radiocarbon* 52, 103–112. <https://doi.org/10.1017/S0033822200045069>.
- Brück, J., 1999. Ritual and rationality: some problems of interpretation in European archaeology. *Eur. J. Archaeol.* 2, 313–344.
- Bruzek, J., 2002. A method for visual determination of sex, using the human hip bone. *Am. J. Phys. Anthropol.* 117, 157–168. <https://doi.org/10.1002/ajpa.10012>.
- Caine, J.S., Evans, J.P., Forster, C.B., 1996. Fault zone architecture and permeability structure. *Geology* 24, 1025–1028. [https://doi.org/10.1130/0091-7613\(1996\)024<1025:FZAAPS>2.3.CO;2](https://doi.org/10.1130/0091-7613(1996)024<1025:FZAAPS>2.3.CO;2).
- Calcagnile, L., Maruccio, L., Scrimieri, L., delle Side, D., Braione, E., D'Elia, M., Quarta, G., 2019. Development and application of facilities at the centre for applied physics, dating and diagnostics (CEDAD) at the university of Salento during the last 15 years. *Nucl. Instrum. Methods Phys. Res. Sect. B Beam Interact. Mater. Atoms* 456, 252–256. <https://doi.org/10.1016/j.nimb.2019.03.031>.
- Cancellieri, M., 1986. Le vie d'acqua dell'area pontina. *Archeol. Laz* VII, 143–156.
- Carboni, G., 2002. Territorio aperto o di frontiera? Nuove prospettive di ricerca per lo studio della distribuzione spaziale delle facies del Gaudio e di Rinaldone nel Lazio centro-meridionale. *Origini XXIV* 235–299.
- Carboni, G., 2019. "Territorio Aperto o di Frontiera?" quindici anni dopo. Conferme e nuove evidenze dell'età del Rame nel Lazio centro-meridionale. *IpoTESI di Preist* 11. <https://doi.org/10.6092/issn.1974-7985/9899>.
- Cardello, G.L., Doglioni, C., 2015. From mesozoic rifting to apennine orogeny: the gran sasso range (Italy). *Gondwana Res.* 27, 1307–1334. <https://doi.org/10.1016/j.jgr.2014.09.009>.
- Cardello, G.L., Mancktelow, N.S., 2014. Cretaceous syn-sedimentary faulting in the wildhorn nappes (SW Switzerland). *Swiss J. Geosci.* 107, 223–250. <https://doi.org/10.1007/s00015-014-0166-8>.
- Cardello, G.L., Mancktelow, N.S., 2015. Veining and post-nappe transtensional faulting in the SW Helvetic Alps (Switzerland). *Swiss J. Geosci.* 108, 379–400. <https://doi.org/10.1007/s00015-015-0199-7>.
- Cardello, G.L., Tesei, T., 2013. Transtensive faulting in carbonates at different crustal levels: examples from SW Helvetic and Central Apennines. *Rendiconti online della Società Geologica Italiana* 29, 20–23. <https://doi.org/10.3301/GFT.2016.04>. Socgeol.net.
- Cardello, G.L., Di Vincenzo, G., Giorgetti, G., Zwingmann, H., Mancktelow, N., 2019. Initiation and development of the Pennine Basal Thrust (Swiss Alps): a structural and geochronological study of an exhumed megathrust. *J. Struct. Geol.* 126, 338–356. <https://doi.org/10.1016/j.jsg.2019.06.014>.
- Cardello, G.L., Consorti, L., Palladino, D.M., Carminati, E., Carlini, M., Doglioni, C., 2020. Tectonically controlled carbonate-seated maar-diatreme volcanoes: the case of the Volsci Volcanic Field, central Italy. *J. Geodyn.* 139, 101763. <https://doi.org/10.1016/j.jog.2020.101763>.
- Cardello, G.L., Vico, G., Consorti, L., Sabbatino, M., Carminati, E., Doglioni, C., 2021. Constraining the passive to active margin tectonics of the internal central Apennines: insights from biostratigraphy, structural, and seismic analysis. *Geosciences* 11 (4), 160. <https://doi.org/10.3390/geosciences11040160>.
- Carminati, E., Lustrino, M., Doglioni, C., 2012. Geodynamic evolution of the central and western Mediterranean: tectonics vs. igneous petrology constraints. *Tectonophysics* 579, 173–192. <https://doi.org/10.1016/j.tecto.2012.01.026>.
- Casini, L., Andreucci, S., Sechi, D., Huang, C.-Y., Shen, C.-C., Pascucci, V., 2020. Luminescence dating of Late Pleistocene faults as evidence of uplift and active tectonics in Sardinia, W Mediterranean. *Terra. Nova* 32, 261–271. <https://doi.org/10.1111/ter.12458>.
- Castagnino Berlinghieri, E.F., Antonioli, F., Bailey, G., 2020. Italy: the archaeology of palaeoshorelines, coastal caves and seafaring connections. In: Bailey, G., Galanidou, N., Peeters, H., Jöns, H., Mennenga, M. (Eds.), *The Archaeology of Europe's Drowned Landscapes*. Springer International Publishing, Cham, pp. 321–340. https://doi.org/10.1007/978-3-030-37367-2_16.
- Cavazzuti, C., Skeates, R., Millard, A.R., Nowell, G., Peterkin, J., Bernabò Brea, M., Cardarelli, A., Salzani, L., 2019. Flows of people in villages and large centres in Bronze Age Italy through strontium and oxygen isotopes. *PLoS One* 14, e0209693.
- Cazarin, C.L., Bezerra, F.H.R., Borghi, L., Santos, R.V., Favoreto, J., Brod, J.A., Auler, A.S., Srivastava, N.K., 2019. The conduit-seal system of hypogene karst in Neoproterozoic carbonates in northeastern Brazil. *Mar. Petrol. Geol.* 101, 90–107. <https://doi.org/10.1016/j.marpetgeo.2018.11.046>.
- Cazzella, A., Guidi, A., 2016. Aspetti simbolici connessi con le grotte nell'Italia centro-meridionale dal Neolitico alla prima età del ferro. *Quad. di Stud. e Mater. di Stor. delle Religi.* suppl. 82, 47–63.
- Centamore, E., Di Manna, P., Rossi, D., 2007. Kinematic evolution of the Volsci Range: a new overview. *Boll. della Soc. Geol. Ital.* 126, 159–172.
- Centamore, E., Dramis, F., Di Manna, P., Fumanti, F., M., S., Rossi, D., Palombo, M.R., Palladino, D.M., Trigila, R., Zanon, V., Chiocchini, M., Didaskalou, P., Potetti, M., Nisio, S., 2010. Note illustrative del Foglio 402 Ceccano. *Carta Geologica d'Italia 1:50.000. Servizio Geologico d'Italia (Firenze)*.
- Chiarabba, C., Amato, A., Anselmi, M., Baccheschi, P., Bianchi, I., Cattaneo, M., Cecere, G., Chiaraluze, L., Ciaccio, M.G., De Gori, P., De Luca, G.I., Di Bona, M., Di Stefano, R., Faenza, L., Govoni, A., Improta, L., Lucente, F.P., Marchetti, A., Margheriti, L., Mele, F., Michelini, A., Monachesi, G., Moretti, M., Pastori, M., Piana Agostinetti, N., Piccinini, D., Roselli, P., Seccia, D., Valoroso, L., 2009. The 2009 L'Aquila (central Italy) MW6.3 earthquake: main shock and aftershocks. *Geophys. Res. Lett.* 36 (18) <https://doi.org/10.1029/2009GL039627>.
- Clemenzi, L., Storti, F., Balsamo, F., Molli, G., Ellam, R., Muecher, P., Swennen, R., 2015. Fluid pressure cycles, variations in permeability, and weakening mechanisms along low-angle normal faults: the Tellaro detachment, Italy. *GSA Bulletin* 127 (11–12), 1689–1710.
- Cocchi Genick, D., 1995. La facies di Grotta Nuova. In: *Cocchi Genick, D. (Ed.), Aspetti Culturali Della Media Età Del Bronzo In Italia Centro-Meridionale*, pp. 364–397.
- Cocchi Genick, D., 1998. L'antica età del Bronzo nell'Italia centrale. *Profilo di un'epoca e di un'appropriata strategia metodologica* (Firenze).
- Cocchi Genick, D., 2002. *Grotta Nuova: la prima unità culturale attorno all'Etruria protostorica*. M. Baroni, Viareggio Lucca [Italy].
- Consorti, L., Frijia, G., Caus, E., 2017. Rotaloidean foraminifera from the Upper Cretaceous carbonates of Central and Southern Italy and their chronostratigraphic age. *Cretac. Res.* 70, 226–243. <https://doi.org/10.1016/>

- j.cretres.2016.11.004.
- Cosentino, D., Cipollari, P., Di Donato, V., Sgrosso, I., 2002. The Volsci Range in the kinematic evolution of the northern and southern Apennine orogenic system. *Ital. J. Geosci. Volume spe* 209–218.
- Cuffaro, M., Martorelli, E., Bosman, A., Conti, A., Bigi, S., Muccini, F., Cocchi, L., Ligi, M., Bortoluzzi, G., Scrocca, D., Canese, S., Chiocci, F.L., Conte, A.M., Dogliani, C., Perinelli, C., 2016. The ventotene volcanic ridge: a newly explored complex in the central Tyrrhenian Sea (Italy). *Bull. Volcanol.* 78, 86. <https://doi.org/10.1007/s00445-016-1081-9>.
- Curzi, M., Billi, A., Carminati, E., Rossetti, F., Albert, R., Aldega, L., Cardello, G.L., Conti, A., Gerdes, A., Smeraglia, L., Van der Lelij, R., Vignaroli, G., Viola, G., 2020. Disproving the presence of Palaeozoic-Triassic metamorphic rocks on the Island of Zannone (central Italy): implications for the early stages of the Tyrrhenian-Apennines tectonic evolution. *Tectonics* N/a, e2020TC006296. <https://doi.org/10.1029/2020TC006296>.
- Dal Zilio, L., van Dinther, Y., Gerya, T.V., Pranger, C.C., 2018. Seismic behaviour of mountain belts controlled by plate convergence rate. *Earth Planet Sci. Lett.* 482, 81–92.
- Damiani, I., 1995. La facies protoappenninica. In: Cocchi Genick, D. (Ed.), *Aspetti Culturali Della Media Età Del Bronzo in Italia Centro-Meridionale*, pp. 398–428.
- Davies, W., 1988. *Small Worlds: the Village Community in Early Medieval Brittany*. University of California Press, Berkeley.
- Dee, M.W., Palstra, S.W.L., Aerts-Bijma, A.T., Bleeker, M.O., de Bruijn, S., Ghebru, F., Jansen, H.G., Kuitens, M., Paul, D., Richie, R.R., Spriensma, J.J., Scifo, A., van Zonneveld, D., Verstappen-Dumoulin, B.M.A.A., Wietzes-Land, P., Meijer, H.A.J., 2019. Radiocarbon dating at gronings: new and updated chemical pretreatment procedures. *Radiocarbon* 62, 63–74. <https://doi.org/10.1017/RDC.2019.101>.
- Delchiaro, M., Fioramonti, V., Della Seta, M., Cavinato, G.P., Mattei, M., 2020. Fluvial inverse modelling for inferring the timing of Quaternary uplift in the Simbruini range (Central Apennines, Italy). In: Massimiliano, A., Marchesini, I., Melelli, L., Guth, P. (Eds.), *Proceedings of the Geomorphometry 2020 Conference*. https://doi.org/10.30437/GEOMORPHOMETRY2020_58.
- Dennel, R.W., Webley, D., 1975. In: Higgs, E.S. (Ed.), *Prehistoric Settlement and Land Use in Southern Bulgaria, Palaeoeconomy*. Cambridge University Press, Cambridge, pp. 97–109. <https://doi.org/10.1017/S0079497X00011026>.
- Di Domenica, A., Pizzi, A., 2017. Defining a mid-Holocene earthquake through speleoseismological and independent data: implications for the outer Central Apennines (Italy) seismotectonic framework. *Solid Earth* 8, 161–176. <https://doi.org/10.5194/se-8-161-2017>.
- Dogliani, C., Barba, S., Carminati, E., Riguzzi, F., 2015. Fault on-off versus strain rate and earthquakes energy. *Geosci. Front.* 6 (2), 265–276.
- Drechsler-Bizic, R., 1980. Bronze age necropolis in the cave Bezdanjaca near Vrhovine. *Bull. Arch. Museum Zagreb* 3/XIII-XII, 27–28.
- Dunbar, R.I.M., 1996. *Grooming, Gossip, and the Evolution of Language*. Faber and Faber Limited.
- Ekmeççi, M., 2003. Review of Turkish karst with special emphasis on tectonic and climatic controls. *Acta Carsol.* 32, 205–218.
- Ekmeççi, M., 2005. Karst in Turkish thrace: compatibility between geological history and karst type. *Turk. J. Earth Sci.*
- Ellison, A., Harriss, J., 1974. Settlement and land use in the prehistory and early history of southern England: a study based on locational models. In: Clarke, D.L. (Ed.), *Models in Archaeology*. Methuen, London, pp. 911–962.
- Ennes-Silva, R.A., Bezerra, F.H.R., Nogueira, F.C.C., Balsamo, F., Klimchouk, A., Cazarin, C.L., Auler, A.S., 2016. Superposed folding and associated fracturing influence hypogene karst development in Neoproterozoic carbonates, São Francisco Craton, Brazil. *Tectonophysics* 666, 244–259. <https://doi.org/10.1016/j.tecto.2015.11.006>.
- Falucci, E., Gori, S., Galadini, F., Fubelli, G., Moro, M., Saroli, M., 2016. Active faults in the epicentral and mesoseismal Ml 6.0 24, 2016 Amatrice earthquake region, central Italy. *Methodological and seismotectonic issues*. *Ann. Geophys.* 59.
- Farina, S., 2011. Late pleistocene-holocene mammals from “canale delle Acque Alte (canale mussolini)” (agro pontino, Latium). *Boll. della Soc. Paleontol. Ital.* 50, 11–22.
- Faure Walker, J., Boncio, P., Pace, B., Roberts, G., Benedetti, L., Scotti, O., Visini, F., Peruzza, L., 2020. Fault2SHA Central Apennines Database. Institute for Risk and Disaster Reduction. PANGAEA. <https://doi.org/10.1594/PANGAEA.922582>.
- Ferranti, L., Antonioli, F., Mauz, B., Amorosi, A., Dai Pra, G., Mastronuzzi, G., Monaco, C., Orrù, P., Pappalardo, M., Radtke, U., Renda, P., Romano, P., Sansò, P., Verrubbi, V., 2006. Markers of the last interglacial sea-level high stand along the coast of Italy: tectonic implications. *Quat. Int.* 145–146, 30–54. <https://doi.org/10.1016/j.quaint.2005.07.009>.
- Ferranti, L., Pace, B., Vasta, M., Colella, A., Ramondini, M., Calcaterra, D., Di Bianco, S., Valentini, A., De Massis, J., Teodoro, P., Berardi, D., La Rocca, N., 2015. Evaluation of the seismogenic potential in key areas of the central and southern Apennines through analysis of speleothem vulnerability. In: 6th International INQUA Meeting on Paleoseismology, Active Tectonics and Archaeoseismology.
- Fiorillo, A., 2016. Il rapporto uomo-orso nelle grotte italiane del tardo Pleistocene. Università degli Studi di Roma Tor Vergata.
- Flannery, K.V., 1976. *The Early Mesoamerican Village*. Academic Press, New York.
- Forge, A., 1972. Normative factors in the settlement size of neolithic cultivators (New Guinea). In: Ucko, P.J., Dimbleby, G.W., Tringham, R. (Eds.), *Man, Settlement and Urbanism* (London).
- Forti, P., Postpischl, D., 1984. Seismotectonic and paleoseismic analyses using karst sediments. *Mar. Geol.* 55, 145–161. [https://doi.org/10.1016/0025-3227\(84\)90138-5](https://doi.org/10.1016/0025-3227(84)90138-5).
- Frepoli, A., Cimini, G.B., De Gori, P., De Luca, G., Marchetti, A., Monna, S., Montuori, C., Pagliuca, N.M., 2017. Seismic sequences and swarms in the Latium-Abruzzo-Molise Apennines (central Italy): new observations and analysis from a dense monitoring of the recent activity. *Tectonophysics* 712–713, 312–329. <https://doi.org/10.1016/j.tecto.2017.05.026>.
- Fukasawa, K., Akasaka, T., 2019. Long-lasting effects of historical land use on the current distribution of mammals revealed by ecological and archaeological patterns. *Sci. Rep.* 9, 10697. <https://doi.org/10.1038/s41598-019-46809-1>.
- Galadini, F., Galli, P., 2000. Active tectonics in the central Apennines (Italy) – input data for seismic hazard assessment. *Nat. Hazards* 22, 225–268. <https://doi.org/10.1023/A:1008149531980>.
- Galadini, F., Messina, P., 2004. Early–middle Pleistocene eastward migration of the abruzzu apennine (central Italy) extensional domain. *J. Geodyn.* 37 (1), 57–81.
- Galli, P., 2020. Recurrence times of central-southern Apennine faults (Italy): hints from palaeoseismology. *Terra Nova*. <https://doi.org/10.1111/ter.12470> n/a.
- Gatta, M., Rolfo, M.F., 2017. Cava Muracci: a new middle-upper palaeolithic site in west-central Italy. *Mediterr. Archaeol. Archaeom.* 17, 105–116. <https://doi.org/10.5281/zenodo.581729>.
- Gatta, M., Sinopoli, G., Giardini, M., Giaccio, B., Hajdas, I., Pandolfi, L., Bailey, G., Spikins, P., Rolfo, M.F., Sadori, L., 2016. Pollen from Late Pleistocene hyena (Crocota crocata spelaea) coprolites: an interdisciplinary approach from two Italian sites. *Rev. Palaeobot. Palynol.* 233, 56–66. <https://doi.org/10.1016/j.jrevpalbo.2016.07.005>.
- Gatta, M., Kotsakis, T., Pandolfi, L., Petronio, C., Salari, L., Achino, K.F., Silvestri, L., Rolfo, M.F., 2019. The late Pleistocene faunal assemblage from Cava Muracci (Latium, Italy): palaeoenvironmental implications for coastal central Italy during MIS 3. *Comptes Rendus Palevol* 18, 51–71. <https://doi.org/10.1016/j.crpv.2018.04.006>.
- Goepfert, N., Goldscheider, N., Scholz, H., 2011. Karst geomorphology of carbonatic conglomerates in the folded molasse zone of the northern Alps (Austria/Germany). *Geomorphology* 130, 289–298. <https://doi.org/10.1016/j.geomorph.2011.04.011>.
- Goldscheider, N., 2005. Fold structure and underground drainage pattern in the alpine karst system Hochifien-Gottesacker. *Eclogae Geol. Helv.* 98, 1–17. <https://doi.org/10.1007/s00015-005-1143-z>.
- Gomez de Soto, J., 1973. La grotte sépulcrale des Duffaits (La Rochette, Charente). *Bull. la Société Préhistorique Française* 70, 401–444.
- Guidi, A., 1992. Recenti ritrovamenti in grotta nel Lazio: un riesame critico del problema dell'utilizzazione delle cavità naturali. *Rass. di Archeol. X*, 427–437.
- Guidi, A., Rosini, L., 2019. *Materiali protostorici dalla grotta Vittorio Vecchi (sezze romano, LT)*, 2919. BAR International Series, Oxford.
- Religion and ritual. In: Harding, A.F. (Ed.), 2000. *European Societies in the Bronze Age*, Cambridge World Archaeology. Cambridge University Press, Cambridge, pp. 308–351. <https://doi.org/10.1017/CBO9780511605901.010>.
- Heidinga, H.A., 1987. Medieval settlement and economy north of the lower rhine. In: *Archaeology and History of Kootwijk and the Veluwe (the Netherlands)*. Van Gorcum, Assen-Maastricht.
- Higham, T.F.G., Jacobi, R.M., Ramsey, C.B., 2006. AMS radiocarbon dating of ancient bone using ultrafiltration. *Radiocarbon* 48, 179–195. <https://doi.org/10.1017/S0033822200066388>.
- Houdaille, J., Acsadi, G., Nemeskeri, J., 1972. History of human life span and mortality. *Ann. Demogr. Hist., Paris*, pp. 377–379.
- Hughes, P.D., Woodward, J.C., 2008. Timing of glaciation in the Mediterranean mountains during the last cold stage. *J. Quat. Sci.* 23, 575–588. <https://doi.org/10.1002/jqs.1212>.
- İşcan, Y., 1985. Osteometric analysis of sexual dimorphism in the sternal end of the rib. *J. Forensic Sci.* 30, 1090–1099. <https://doi.org/10.1520/JFS11050J>.
- Karner, D.B., Marra, F., Florindo, F., Boschi, E., 2001. Pulsed uplift estimated from terrace elevations in the coast of Rome: evidence for a new phase of volcanic activity? *Earth Planet Sci. Lett.* 188, 135–148.
- Klimchouk, A., Ford, D., 2000. Lithologic and structural controls of dissolutional cave development. In: Klimchouk, A., Ford, D.C., Palmer, A.N., Dreybrodt, W. (Eds.), *Speleogenesis. Evolution of Karst Aquifers*. National Speleological Society, pp. 54–64.
- Klimchouk, A., Tymokhina, E., Amelichev, G., 2012. Speleogenetic effects of interaction between deeply derived fracture-conduit flow and intrastratal matrix flow in hypogene karst settings. *Int. J. Speleol.* 41, 161–179. <https://doi.org/10.5038/1827-806X.41.2.4>.
- Klimchouk, A., Auler, A.S., Bezerra, F.H.R., Cazarin, C.L., Balsamo, F., Dublyansky, Y., 2016. Hypogenic origin, geologic controls and functional organization of a giant cave system in Precambrian carbonates, Brazil. *Geomorphology* 253, 385–405. <https://doi.org/10.1016/j.geomorph.2015.11.002>.
- Langmuir, E., 1984. *Mountaincraft and Leadership*. The Scottish Sports Council/MLTB, Cordee, Leicester.
- Lewin, R., 1992. *Complexity. Life at the Edge of Chaos*. Macmillan Pub. Co., New York.
- Locati, M., Camassi, R., Rovida, A., Ercolani, E., Bernardini, F., Castelli, V., Caracciolo, C.H., Tertulliani, A., Rossi, A., Azzaro, R., D'Amico, S., Antonucci, A., 2021. Database Macrosismico Italiano (DBMI15), Versione 3.0. Istituto Nazionale di Geofisica e Vulcanologia (INGV). <https://doi.org/10.13127/DBMI/DBMI15.3>.
- Lovejoy, C.O., Meindl, R.S., Pryzbeck, T.R., Mensforth, R.P., 1985. Chronological metamorphosis of the auricular surface of the ilium: a new method for the determination of adult skeletal age at death. *Am. J. Phys. Anthropol.* 68, 15–28. <https://doi.org/10.1002/ajpa.13306808103>.
- Macchiarella, I., 1995. La facies appenninica. In: Cocchi Genick, D. (Ed.), *Aspetti*

- Culturali Della Media Età Del Bronzo in Italia Centro-Meridionale, pp. 441–463.
- Marra, F., Florindo, F., Anzidei, M., Sepe, V., 2016. Paleo-surfaces of glacio-eustatically forced aggradational successions in the coastal area of Rome: assessing interplay between tectonics and sea-level during the last ten interglacials. *Quat. Sci. Rev.* 148, 85–100. <https://doi.org/10.1016/j.quascirev.2016.07.003>.
- Marra, F., Gaeta, M., Jicha, B.R., Nicosia, C., Tolomei, C., Ceruleo, P., Florindo, F., Gatta, M., La Rosa, M., Rolfo, M.F., 2019a. MIS 9 to MIS 5 terraces along the Tyrrhenian Sea coast of Latium (central Italy): assessing interplay between sea-level oscillations and tectonic movements. *Geomorphology* 346, 106843. <https://doi.org/10.1016/j.geomorph.2019.106843>.
- Marra, F., Bahain, J.-J., Jicha, B.R., Nomade, S., Palladino, D.M., Pereira, A., Tolomei, C., Voinchet, P., Anzidei, M., Aureli, D., Ceruleo, P., Falguères, C., Florindo, F., Gatta, M., Ghaleb, B., La Rosa, M., Peretto, C., Petronio, C., Rocca, R., Rolfo, M.F., Salari, L., Smedile, A., Tombret, O., 2019b. Reconstruction of the MIS 5.5, 5.3 and 5.1 coastal terraces in Latium (central Italy): a re-evaluation of the sea-level history in the Mediterranean Sea during the last interglacial. *Quat. Int.* 525, 54–77. <https://doi.org/10.1016/j.quaint.2019.09.001>.
- Marra, F., Rolfo, F.M., Gaeta, M., Florindo, F., 2020. Anomalous last interglacial Tyrrhenian Sea levels and neanderthal settling at Guattari and moscerini caves (central Italy). *Sci. Rep.* 10, 11929. <https://doi.org/10.1038/s41598-020-68604-z>.
- Marra, F., Cardello, G.L., Gaeta, M., Jicha, B.R., Montone, P., Niespolo, E.M., Nomade, S., Palladino, D.M., Pereira, A., De Luca, G., Florindo, F., Frepoli, A., Renne, P.R., Sottili, G., 2021. The Volsci Volcanic Field (central Italy): eruptive history, magma system and implications on continental subduction processes. *Int. J. Earth Sci.* <https://doi.org/10.1007/s00531-021-01981-6>.
- Meindl, R.S., Lovejoy, C.O., Mensforth, R.P., Walker, R.A., 1985. A revised method of age determination using the os pubis, with a review and tests of accuracy of other current methods of public symphyseal aging. *Am. J. Phys. Anthropol.* 68, 29–45. <https://doi.org/10.1002/ajpa.1330680104>.
- Menant, A., Angiboust, S., Gerya, T., 2019. Stress-driven fluid flow controls long-term megathrust strength and deep accretionary dynamics. *Sci. Rep.* 9 (1), 1–11.
- Milia, A., Torrente, M.M., 2015. Tectono-stratigraphic signature of a rapid multistage subsiding rift basin in the Tyrrhenian-Apennine hinge zone (Italy): a possible interaction of upper plate with subducting slab. *J. Geodyn.* 86, 42–60. <https://doi.org/10.1016/j.jog.2015.02.005>.
- Miller, T.E., 1996. Geologic and hydrologic controls on karst and cave development in Belize. *J. Cave Karst Stud.* 58, 100–120.
- Montone, P., Mariucci, M.T., 2016. The new release of the Italian contemporary stress map. *Geophys. J. Int.* 205 (3), 1525–1531. <https://doi.org/10.1093/gji/ggw100>.
- Montone, P., Amato, A., Pondrelli, S., 1999. Active stress map of Italy. *J. Geophys. Res.: Solid Earth* 104 (B11), 25595–25610.
- Mook, W.G., Streumar, H.J., 1983. Physical and chemical aspects of radiocarbon dating. *PACT* 8, 45–53.
- Morley, C.K., Nelson, R.A., Patton, T.L., Munn, S.G., 1990. Transfer zones in the East African rift system and their relevance to hydrocarbon exploration in rifts. *AAPG Bull.* 74 (8), 1234–1253.
- Naismith, W.W., 1892. Excursions. Cruach ardran, stobinian, and ben more. *Scottish Mountain Club J.* 2, 136.
- Orschiedt, J., 2012. Cave burials in prehistoric central Europe. In: Bergsvik, A.K., Skeates, R. (Eds.), *Caves in Context. The Cultural Significance of Caves and Rockshelters in Europe*. Oxbow books, pp. 212–224.
- Ortner, H., Reiter, F., Acs, P., 2002. Easy handling of tectonic data: the programs TectonicVB for mac and TectonicsFP for Windows™. *Comput. Geosci.* 28, 1193–1200. [https://doi.org/10.1016/S0098-3004\(02\)00038-9](https://doi.org/10.1016/S0098-3004(02)00038-9).
- Pacciarelli, M., 2001. Dal villaggio alla città. La svolta protourbana del 1000 a.C. nell'Italia tirrenica (Firenze).
- Pace, B., Valentini, A., Ferranti, L., Vasta, M., Vassallo, M., Montagna, P., Colella, A., Pons-Branchu, E., 2020. A large paleoearthquake in the central Apennines, Italy, recorded by the collapse of a cave speleothem. *Tectonics* 39. <https://doi.org/10.1029/2020TC006289>.
- Pepe, M., Parise, M., 2014. Structural control on development of karst landscape in the Salento Peninsula (Apulia, SE Italy). *Acta Carsol.* 43 <https://doi.org/10.3986/ac.v43i1.643>.
- Perfettini, H., Avouac, J.P., Tavera, H., Kositsky, A., Nocquet, J.M., Bondoux, F., Chlieh, M., Sladen, A., Audin, L., Farber, L.H., Soler, P., 2010. Seismic and aseismic slip on the Central Peru megathrust. *Nature* 465 (7294), 78.
- Perles, C., 1999. In: Halstead, P. (Ed.), *The Distribution of Magoules in Eastern Thessaly, Neolithic Society in Greece*, pp. 42–56.
- Petronio, C., Di Canzio, E., Salari, L., 2007. The Late Pleistocene and Holocene Mammals in Italy: new biochronological and paleoenvironmental data. *Palaeontograph. Abteilung* 279, 147–157. <https://doi.org/10.1127/pala/279/2007/147>.
- Pisani, L., Antonellini, M., De Waele, J., 2019. Structural control on epigenic gypsum caves: evidences from Messinian evaporites (Northern Apennines, Italy). *Geomorphology* 332, 170–186. <https://doi.org/10.1016/j.geomorph.2019.02.016>.
- Postpischil, D., Agostini, S., Forti, P., Quinif, Y., 1991. Palaeoseismicity from karst sediments: the "Grotta del Cervò" cave case study (Central Italy). *Tectonophysics* 193, 33–44. [https://doi.org/10.1016/0040-1951\(91\)90186-V](https://doi.org/10.1016/0040-1951(91)90186-V).
- Pounds, N.J.G., 1974. *An Economic History of Medieval Europe*. Longman, London ; New York.
- Rappaport, R.A., 1999. *Ritual and Religion in the Making of Humanity*. Cambridge University Press, Cambridge.
- Rawling, G.C., Goodwin, L.B., Wilson, J.L., 2001. Internal architecture, permeability structure, and hydrologic significance of contrasting fault-zone types. *Geology* 29, 43–46. [https://doi.org/10.1130/0091-7613\(2001\)029<0043:IAPSAH>2.0.CO;2](https://doi.org/10.1130/0091-7613(2001)029<0043:IAPSAH>2.0.CO;2).
- Reimer, P.J., Bard, E., Bayliss, A., Beck, J.W., Blackwell, P.G., Bronk Ramsey, C., Buck, C.E., Cheng, H., Edwards, R.L., Friedrich, M., Grootes, P.M., Guilderson, T.P., Haffidason, H., Hajdas, I., Hatté, C., Heaton, T.J., Hoffmann, D.L., Hogg, A.G., Hughen, K.A., Kaiser, K.F., Kromer, B., Manning, S.W., Niu, M., Reimer, R.W., Richards, D.A., Scott, E.M., Southon, J.R., Staff, R.A., Turney, C.S.M., Van der Plicht, J., 2013. IntCal13 and Marine13 radiocarbon age calibration curves 0–50,000 years cal BP. *Radiocarbon* 55, 1869–1887.
- Ricciardi, A.B., 2012. Utilizzazione delle cavità naturali dell'Italia centrale nell'età del Bronzo. Università degli Studi Roma Tre.
- Rick, T.C., Sandweiss, D.H., 2020. Archaeology, climate, and global change in the Age of Humans. *Proc. Natl. Acad. Sci. Unit. States Am.* 117, 8250–8253. <https://doi.org/10.1073/pnas.2003612117>.
- Roberts, G.P., Michetti, A.M., 2004. Spatial and temporal variations in growth rates along active normal fault systems: an example from the Lazio–Abruzzo Apennines, central Italy. *J. Struct. Geol.* 26, 339–376. [https://doi.org/10.1016/S0191-8141\(03\)00103-2](https://doi.org/10.1016/S0191-8141(03)00103-2).
- Rovida, A., Locati, M., Camassi, R., Lolli, B., Gasperini, P., 2020. The Italian earthquake catalogue CPTI15. *Bull. Earthq. Eng.* 18, 2953–2984. <https://doi.org/10.1007/s10518-020-00818-y>.
- San Jose, M., Caves Rugenstein, J.K., Cosentino, D., Faccenna, C., Fellin, M.G., Ghinassi, M., Martini, I., 2020. Stable isotope evidence for rapid uplift of the central Apennines since the late Pliocene. *Earth Planet Sci. Lett.* 544, 116376. <https://doi.org/10.1016/j.epsl.2020.116376>.
- Schlagenhauf, A., Manighetti, L., Benedetti, L., Gaudemer, Y., Finkel, R., Malavieille, J., Pou, K., 2011. Earthquake supercycles in Central Italy, inferred from 36Cl exposure dating. *Earth Planet Sci. Lett.* 307, 487–500. <https://doi.org/10.1016/j.epsl.2011.05.022>.
- Serva, L., Brunamonte, F., 2007. Subsidence in the Pontina Plain. Italy. *Bull. Eng. Geol. Environ.* 66, 125–134. <https://doi.org/10.1007/s10064-006-0057-y>.
- Sevink, J., van Gorp, W., Di Vito, M.A., Arienzo, I., 2020. Distal tephra from Campanian eruptions in early late Holocene fills of the agro pontino graben and Fondi basin (southern Lazio, Italy). *J. Volcanol. Geoth. Res.* 107041 <https://doi.org/10.1016/j.jvolgeores.2020.107041>.
- Shanov, S., Kostov, K., 2015. *Dynamic Tectonics and Karst*. Springer-Verlag Berlin Heidelberg. <https://doi.org/10.1007/978-3-662-43992-0>.
- Silva, O.L., Bezerra, F.H.R., Maia, R.P., Cazarin, C.L., 2017. Karst landforms revealed at various scales using LiDAR and UAV in semi-arid Brazil: consideration on karstification processes and methodological constraints. *Geomorphology* 295, 611–630. <https://doi.org/10.1016/j.geomorph.2017.07.025>.
- Silvestri, L., 2017. *Caves and Human Lifeways in Middle Bronze Age Central Italy: a Social Bioarchaeology Approach*. Durham University.
- Silvestri, L., Rolfo, M.F., Angle, M., Skeates, R., Salari, L., 2018. Faunal remains and ritualisation: case studies from Bronze age caves in Central Italy. In: Livarda, A., Magdwick, R., Riera Mora, S. (Eds.), *The Bioarchaeology of Ritual and Religion*. Oxbow Books, Oxford, pp. 129–147.
- Smith, F.A., Elliott Smith, R.E., Lyons, S.K., Payne, J.L., Villaseñor, A., 2019. The accelerating influence of humans on mammalian macroecological patterns over the late Quaternary. *Quat. Sci. Rev.* 211, 1–16. <https://doi.org/10.1016/j.quascirev.2019.02.031>.
- Stafford, K., Mylroie, John, Taborosi, D., Jenson, J., Mylroie, Joan, 2005. Karst development on tinian, commonwealth of the Northern Mariana Islands: controls on dissolution in relation to the carbonate island karst model. *J. Cave Karst Stud.* 67, 14–27.
- Stephens, L., Fuller, D., Boivin, N., Rick, T., Gauthier, N., Kay, A., Marwick, B., Armstrong, C.G., Barton, C.M., Denham, T., Douglass, K., Driver, J., Janz, L., Roberts, P., Rogers, J.D., Thakar, H., Altaweel, M., Johnson, A.L., Sampietro Vattuone, M.M., Aldenderfer, M., Archila, S., Artioli, G., Bale, M.T., Beach, T., Borrell, F., Braje, T., Buckland, P.I., Jiménez Cano, N.G., Capriles, J.M., Diez Castillo, A., Çilingiroğlu, Ç., Negus Cleary, M., Conolly, J., Coutros, P.R., Covey, R.A., Cremaschi, M., Crowther, A., Der, L., di Lernia, S., Doershuk, J.F., Doolittle, W.E., Edwards, K.J., Erlandson, J.M., Evans, D., Fairbairn, A., Faulkner, P., Feinman, G., Fernandes, R., Fitzpatrick, S.M., Fyfe, R., Garcea, E., Goldstein, S., Goodman, R.C., Dalpoim Guedes, J., Herrmann, J., Hiscock, P., Hommel, P., Horsburgh, K.A., Hritz, C., Ives, J.W., Junno, A., Kahn, J.G., Kaufman, B., Kearns, C., Kidder, T.R., Lanoë, F., Lawrence, D., Lee, G.-A., Levin, M.J., Lindskoug, H.B., López-Sáez, J.A., Macrae, S., Marchant, R., Marston, J.M., McClure, S., McCoy, M.D., Miller, A.V., Morrison, M., Motuzaite Matuzeviciute, G., Müller, J., Nayak, A., Noerwidi, S., Peres, T.M., Peterson, C.E., Proctor, L., Randall, A.R., Renette, S., Robbins Schug, G., Ryzewski, K., Saini, R., Scheinsohn, V., Schmidt, P., Sebillaud, P., Seitsonen, O., Simpson, I.A., Sołtyśiak, A., Speakman, R.J., Spengler, R.N., Steffen, M.L., Storzum, M.J., Strickland, K.M., Thompson, J., Thurston, T.L., Ulm, S., Ustunkaya, M.C., Welker, M.H., West, C., Williams, P.R., Wright, D.K., Wright, N., Zahir, M., Zerboni, A., Beaudouin, E., Munevar Garcia, S., Powell, J., Thornton, A., Kaplan, J.O., Gaillard, M.-J., Klein Goldewijk, K., Ellis, E., 2019. Archaeological assessment reveals Earth's early transformation through land use. *Science* 80–(365), 897–902. <https://doi.org/10.1126/science.aax1192>.
- Stiner, M.C., 1991. The faunal remains from grotta Guattari: a taphonomic perspective. *Curr. Anthropol.* 32, 103–117.
- Stucchi, M., Meletti, C., Montaldo, V., Akinci, A., Faccioli, E., Gasperini, P., Malagnini, L., Valensise, G., 2004. Pericolosità sismica di riferimento per il territorio nazionale MPS04 [Data set]. Istituto Nazionale di Geofisica e Vulcanologia (INGV). <https://doi.org/10.13127/sh/mps04/ag>.
- Šušteršič, F., 2006. Relationships between deflector faults, collapse dolines and

- collector channel formation: some examples from Slovenia. *Int. J. Speleol.* 35, 1–12. <https://doi.org/10.5038/1827-806X.35.1.1>.
- Tarquini, S., Isola, I., Favalli, M., Battistini, A., 2007. TINITALY, a Digital Elevation Model of Italy with a 10 M-Cell Size. Istituto Nazionale di Geofisica e Vulcanologia (INGV). <https://doi.org/10.13127/TINITALY/1.0> [Data set], Version 1.0.
- Tîrlă, L., Vijulie, I., 2013. Structural–tectonic controls and geomorphology of the karst corridors in alpine limestone ridges: southern Carpathians, Romania. *Geomorphology* 197, 123–136. <https://doi.org/10.1016/j.geomorph.2013.05.003>.
- Treffort, J.-M., 2005. La fréquentation des cavités naturelles du Jura méridional au Bronze final : état de la question, nouvelles données et perspectives. *Bull. la Société préhistorique française* 401–416.
- Troisi, S., Baiocchi, V., Del Pizzo, S., Giannone, F., 2017. A prompt methodology to georeference complex hypogea environments. *Int. Arch. Photogramm. Remote Sens. Spat. Inf. Sci.* XLII-2/W3 639–644. <https://doi.org/10.5194/isprs-archives-XLII-2-W3-639-2017>.
- Turner, V., 1969. *The Ritual Process*. Aldine, Chicago.
- Ubelaker, D.H., 1989. The estimation of age at death from immature human bone. In: İşcan, Y. (Ed.), *Age Markers in the Human Skeleton*. Charles C. Thomas, Springfield, pp. 55–70.
- van Gorp, W., Sevink, J., 2019. Distal deposits of the Avellino eruption as a marker for the detailed reconstruction of the early Bronze age depositional environment in the agro pontino and Fondi basin (Lazio, Italy). *Quat. Int.* 499B, 245–257. <https://doi.org/10.1016/j.quaint.2018.03.017>.
- van Gorp, W., Sevink, J., van Leusen, P.M., 2020. Post-depositional subsidence of the Avellino tephra marker bed in the Pontine plain (Lazio, Italy): implications for Early Bronze Age palaeogeographical, water level and relative sea level reconstruction. *Catena* 194, 104770. <https://doi.org/10.1016/j.catena.2020.104770>.
- Wells, D.L., Coppersmith, K.J., 1994. New empirical relationships among magnitude, rupture length, rupture width, rupture area, and surface displacement. *Bull. Seismol. Soc. Am.* 84, 974–1002.